12-2017

Experimental Evaluation of Foam-Void Double-Tees

Sachin Sreedhara
Clemson University

Follow this and additional works at: https://tigerprints.clemson.edu/all_theses

EXPERIMENTAL EVALUATION OF FOAM-VOID DOUBLE-TEES

A Thesis
Presented to
the Graduate School of
Clemson University

In Partial Fulfillment
of the Requirements for the Degree
Master of Science
Civil Engineering

by
Sachin Sreedhara
December 2017

Accepted by:
Dr. Brandon Ross, Committee Chair
Dr. Thomas Cousins
Dr. Weichiang Pang

ABSTRACT

Gross vehicular weight restrictions limit the shipping of typical pre-stressed concrete double-tees (DT) for parking decks to one member per trip. The objective of this study is to reduce the self-weight of these members to facilitate two-at-a-time shipping, and thus enable lower shipping costs and reduced environmental footprint. In this research, two 35 foot-long DT members were fabricated and tested to study strategies for reducing self-weight. Foam boards were placed inside the stems of the DT members to produce foam-void double-tees (FVDT). One inch and two inch-thick foam boards were used along with normal and semi-light weight concretes. The two FVDT members were cut length-wise through the top flanges to create four unique single-tee specimens, which were then load tested to evaluate structural capacity and behavior. This thesis discusses the experimental setup and results of flexural testing and shear testing. The test results demonstrated that the presence of foam boards had negligible effect on flexural performance; each of the foam-void specimens supported an experimental moment that was greater than the calculated nominal moment capacity and the shear capacity was more than that expected demand for a typical parking garage DT. Furthermore, cracking near the edges of the foam voids was not an issue under service or higher loads.

DEDICATION

I would like to dedicate this thesis to my beloved parents Mr. Sreedhara Hadya Madappa and Ms. Sudha Malali Lingappa, who have been blessing me all these years, my sisters Ms. Sowmya Praveen, Ms. Shruthi Sreedhara, my brother-in-law Mr. Praveen Puttananjaiah, my beloved advisor Dr. Brandon Ross who has been guiding me since the beginning of my graduate studies and to all my dear friends.

TABLE OF CONTENTS

Table of Contents (Continued)

LIST OF TABLES

LIST OF FIGURES

List of Figures (Continued)

List of Figures (Continued)

I.   INTRODUCTION

Double-Tees (hereafter referred to as "DT") members (Figure 1a) are a staple of the precast concrete industry. Millions of square foot of DT members are fabricated in the United States annually. These members offer flexibility in design and construction, and are an ideal choice for structures such as parking garages that require long uninterrupted spans and high load carrying capability. Because of their widespread use, small improvements in the efficiency of DT members can have a significant effect on the overall environmental footprint and economic competitiveness of the precast industry.

 The Gross Vehicular Weight (GVW) limit for US highways – 80 kip in most states and circumstances – can limit the economical use of DT members. Due to the magnitude of their self-weight, typical 60 ft.-long parking garage DTs cannot be legally transported two per truck. The weight of two parking garage DT members plus the weight of the truck and trailer typically exceeds the Gross Vehicular Weight (GVW) limits by approximately 15%. The current research is motivated by a desire for two-at-a-time transport, which would improve both economic and environmental efficiency. An experimental program was conducted to evaluate the structural viability of foam-void double-tee (FVDT) members (Figure 1b).

Foam voids cast into webs —

Double tee (DT)   Foam-void double tee (FVDT)

(a) Without foam-void   (b) With foam-void
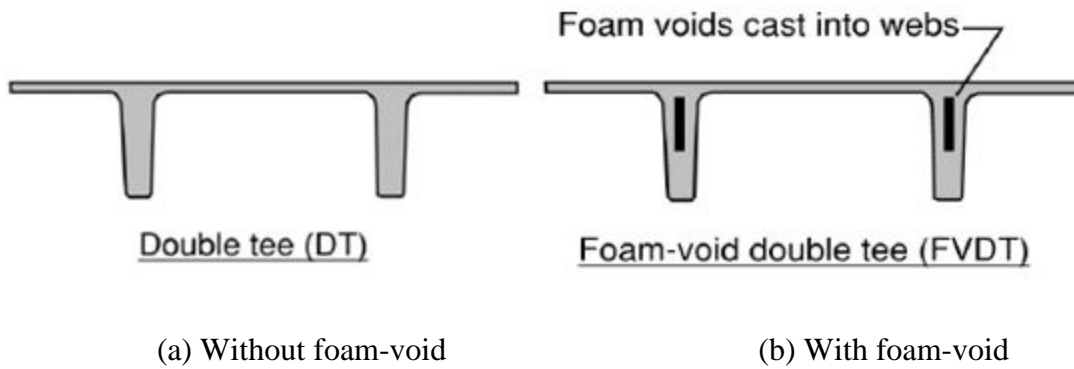
Figure 1. Double Tee cross section

FVDT are similar to typical DT members; however, foam voids are placed in the webs (stems) to displace the concrete and reduce the member weight. Using FVDT in combination with reduced-weight concrete increases the potential for two parking garage double-tees to be trucked simultaneously, thus reducing the economic and environmental costs of transportation. To facilitate these benefits, this study investigated the effect of foam void on service-level cracking behavior, nominal flexural capacity, and shear capacity. Stress, moment, and shear demands on the test specimens were based on a typical precast DT member in a parking garage.

II.   BACKGROUND

Double – Tee Members

Precast pre-tensioned concrete double-tees were first built in 1951. The history of these members in the precast industry has been documented by Nasser et al.[1], Wilden [2], and Edwards [3]. Information in this section is based on these works. The overall form of DT members is well suited for precast concrete construction; standardized cross sections lead to fabrication efficiency and the cross section shape provides structural stability for storage, shipping, erection, and service. The original double-tee cross section (Figure 2, left) has changed and evolved over the years. The cross section has been modified to account for changes in steel and concrete material properties and to suit different loading conditions. Double-tees have been used as floor, roof, and wall structures of buildings and have also been used in industrial applications and in bridges. The New England Extreme Tee (NEXT) beam (Figure 2, right) is being used in highway bridges and is one example of a modern DT member. Parking garages are currently one of (if not the) most common applications of DT members. Parking garage DT members (shown in Figure 1b) are the primary focus of the current research.
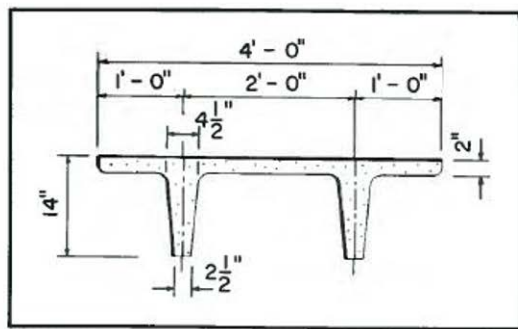
Dimensions of original double-tee.

Figure 2. Early DT (left, figure from Edwards[3]) and NEXT beams (right, photo from

Northeast Precast Products, LLC[4].)

DT members are fabricated as field-topped or factory-topped (Figure 3). Factory-topped DTs have thicker top flanges. Once erected, the flanges act as floor/roof diaphragms. Connections between adjacent factory-topped members are detailed to resist differential vertical movement and to carry diagraph forces. Field-topped members have thinner top flanges and have a concrete topping placed on them after erection. The topping acts compositely with the precast to carry vertical and diaphragm loads. Reinforcement for the diagram is placed in the cast-in-place topping. Field-topped members are commonly used in regions with high seismic loads. The current study focuses exclusively on field-topped DTs.
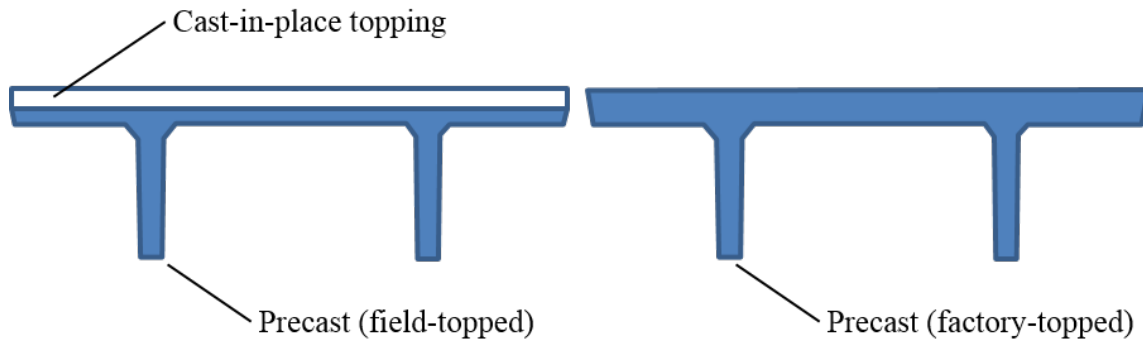
Figure 3. Field-topped (left) and factory-topped (right)

Reduced Weight DTs

Reducing the self-weight of DT members has been the subject of previous research. Barney et al. [5] studied the behavior of the single tee beams with large rectangular openings (Figure 4). They conducted tests on 18 tee beams, having spans of 36 ft and 18 ft. The main variables in the test program were size and location of openings, type and amount of web shear reinforcement and primary flexural reinforcement. The behavior of the beams was observed to be similar to that of a Vierendeel truss (Figure 5). The results showed that the large web openings in the tee beam did not affect the strength or serviceability, so long as the openings were placed outside the required strand embedment length and adequate shear reinforcement was provided adjacent to openings.
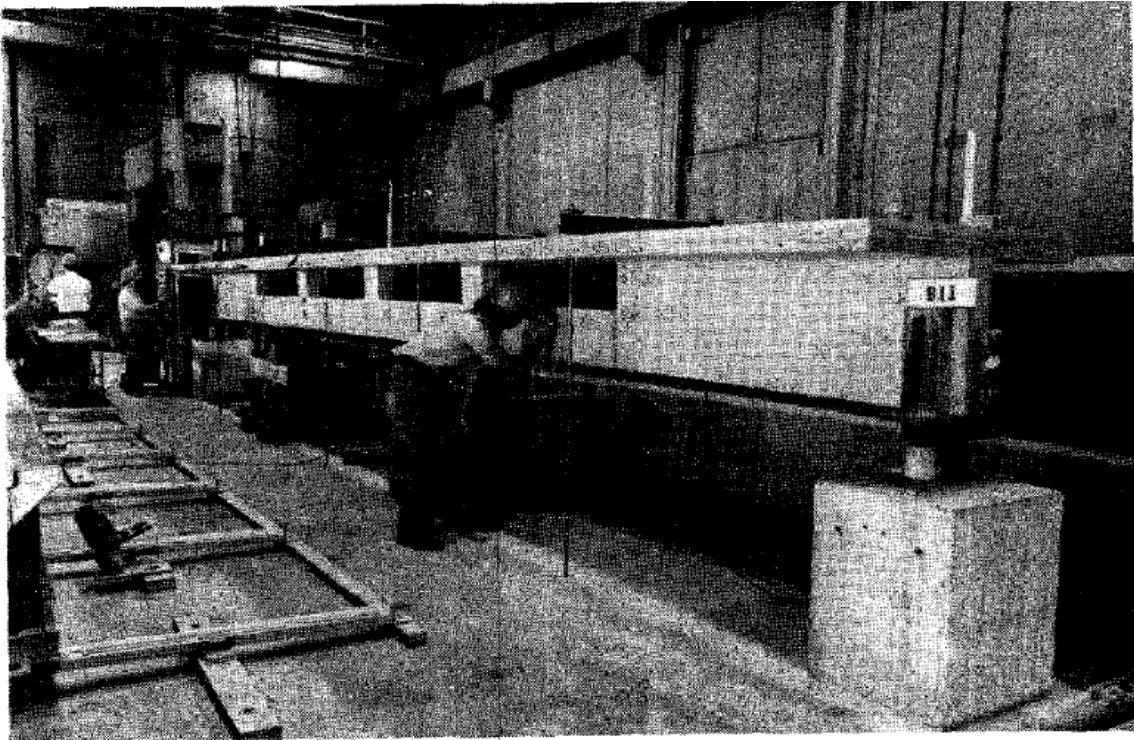
Figure 4. Tee beam with large web openings [5]
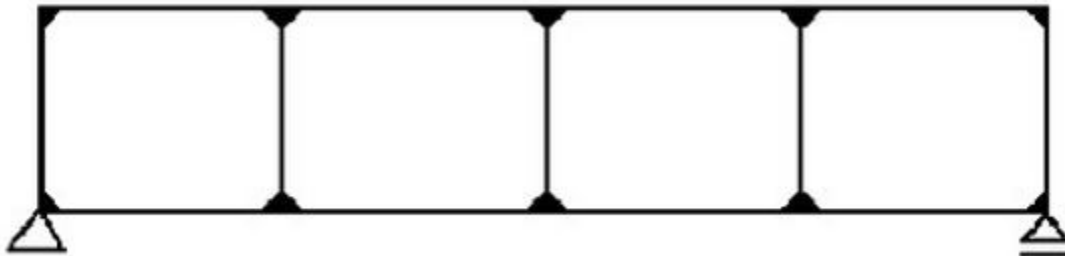
Figure 5. Vierendeel Truss

Savage et al. [6] tested the performance of the prestressed concrete single-tee beams having multiple large web openings (Figure 6). They investigated the opening size, opening placement, required material strengths, and the effect of depressed strands. The test results showed that the performance of the specimens with web openings was

similar to DT members without web openings. Similar to Barney et al., Savage et al. also

observed that specimen behavior was like that of a Vierendeel Truss (Figure 5). It was

also shown that there was no reduction of strength relative to the specimen without

openings, and the deflections were also similar. The ultimate strength of the web-opening

tees was not affected due to the presence of proper reinforcement around the openings.

The deflections were within the ACI requirements.

Figure 6. Single tee with web openings (photo courtesy- M. Tadros)

Saleh et al. [7] optimized the design of double-tee beams with large openings

without reducing the structural capability. This research was the continuation of the work

done by Savage et al. [6]. In order to meet that strength criteria, no openings were placed

at the end of the members within the strand development length. Additional vertical

stirrups at the edges of the openings were provided. Proposed dimensions and

reinforcement details are shown in Figure 7 and Figure 8. The main objective of the

beams with the openings was to reduce the floor to floor heights by using the openings as

chases for electrical and mechanical conduits. Also, because of the openings, the

structural demand due to gravity loads and the effect of seismic forces were reduced.
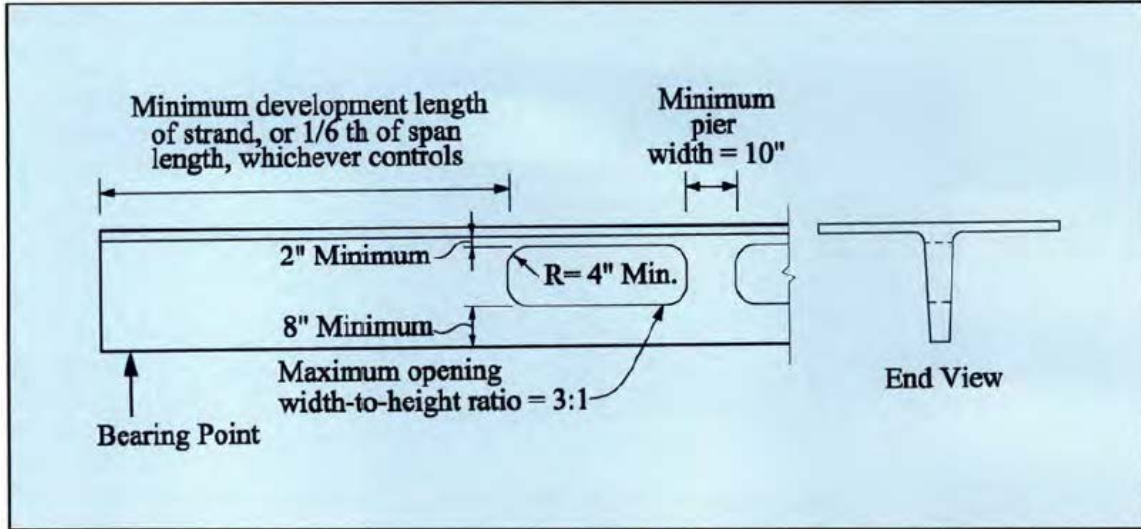
Figure 7. Recommended dimensions and locations of openings in double tee members

(Saleh et al. [7])
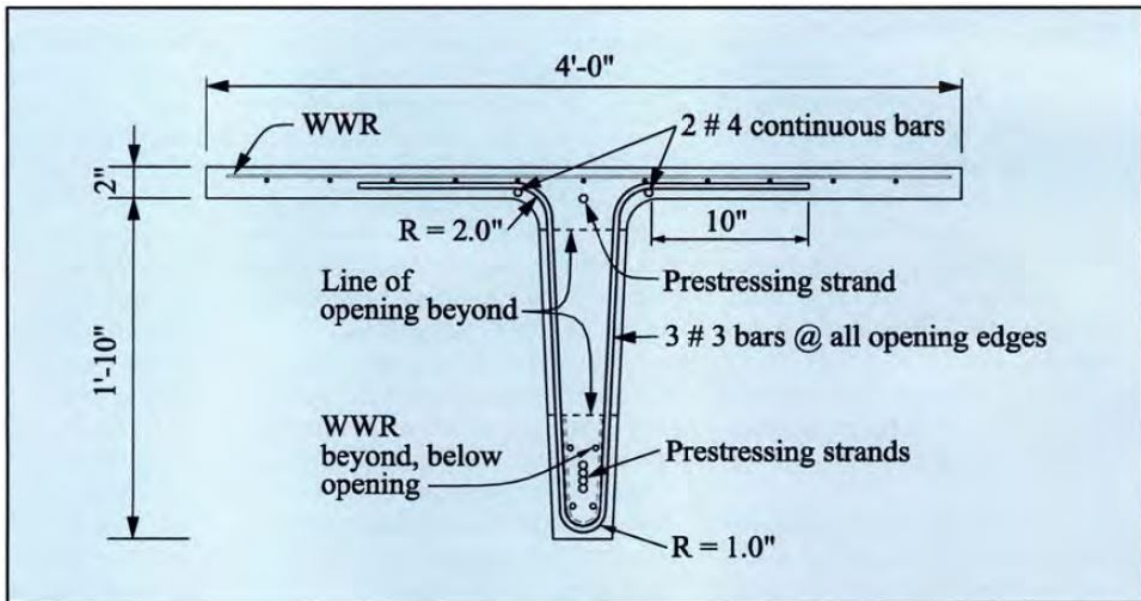
Figure 8. Recommended reinforcement details near edges of openings (Saleh et al. [7])

8

The proprietary BubbleDeck system [8] is another example of reducing structure self-weight by placing voids where concrete is not needed for structural capacity. It is a biaxial technology wherein plastic balls are used to displace the concrete above the reinforcing bars and below the compression zone. Prior to casting the concrete, the plastic balls are held in a prefabricated reinforcing grid. The BubbleDeck system has won numerous awards for its "green" features.

This study expands on the findings of early works through experimentally evaluating the possibility of continuous, outside of the end region, voids in pre-stress/precast concrete beams. The development of FVDT has potential to enhance the precast industry's product lines towards solutions that are competitive in an increasing eco-aware and green construction marketplace.

III.   ESTABLISHMENT OF A "BASELINE" DT MEMBER

Industry Survey

A survey of precast companies was conducted by Srimaruthi Jonnalagadda and Brandon Ross; they provided the results and data which are summarized in this thesis. The survey was conducted to establish a "baseline" design for parking garage DTs. The baseline design mimics typical parking garage DTs, and was used as a point of reference in subsequent research tasks. The survey questionnaire included six questions and requested a shop ticket for a typical parking garage DT. Six US precast fabricators participated in this survey and four of them provided the shop tickets. Questions in the survey asked about typical concrete unit weight, typical concrete strengths (28 day and at transfer), percent of DT members that are field-topped, weight of tractor and trailer shipping DT, truck GVW legal limit in the jurisdiction and trucking cost as percent of total cost for every 100 miles.

Responses are summarized in Table 1. Key observations from the survey include that truck plus trailer weigh between 30 and 35 kips, and that parking garage DT weigh between 30 and 35 kips for normal weight concrete. It is also inferred from the survey data that typically only one parking garage DT is hauled on a truck due to the GVW restrictions. Also, it was noted that some fabricators are using light weight concrete for DT. Using survey responses from the fabricators, properties for a baseline DT member were determined. The self-weight and cross-sectional area of the baseline beam were also established from the survey data, and are reported in Table 2 and Figure 9.

Table 1. Summary of survey, and values for baseline DT member

Item	Range of the response	Value used for baseline
Typical Concrete unit weight	115 – 150 pcf	126 pcf (LWC) 145 pcf (NWC)
Typical Concrete strengths (28 day)	6000 psi	6000 psi
Typical Concrete strength at transfer	3500 – 4000 psi	3500 psi
Percent of DT members that are field topped	60% to 100%	NA
Weight of tractor and trailer shipping DT	30 – 35 kips	32 kips
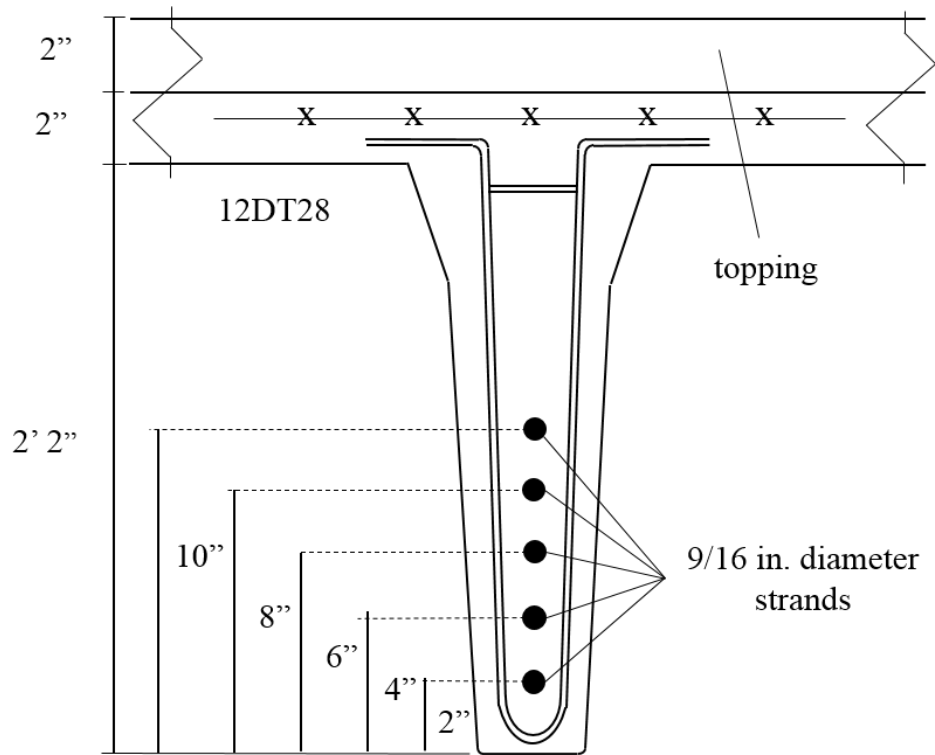
Figure 9. Cross-section of the baseline beam

Table 2. Details of baseline DT

Cross-sectional area	600 in^2
Single DT weight	32.5 kips
Single DT Weight (distributed)	542 plf
Target DT weight after reduction	24 kips

Analysis of baseline DT

In order to fabricate and test FVDT specimens that were comparable to parking garage conditions, the baseline DT was first analyzed to determine service stresses and ultimate shear forces. Baseline DTs with normal-weight and light-weight concrete were considered. The baseline beams were 60 ft long solid (no foam voids) DT with parking garage loading. Details of the baseline cross-section are summarized in Table 3. Loads on the baseline beams included: self-weight, weight of composite topping (25 psf), superimposed dead load (5 psf), and live load (40 psf). Loads were based on ASCE 7-10 [9] and the PCI Design Handbook [10]. Input from the Tindall Corporation was also used to create and analyze the baseline DT design.

Table 3. Summary of the baseline beam cross-section (for one-half of a DT)

Baseline cross-sectional properties	
Area (in^2)	298
S_{top} (in^3)	2754
S_{bottom} (in^3)	1008
P_e (kip)	153
e (in)	14.5
Y_b (in)	20.5

Calculations for the complete analysis (moments, stresses, and shear) are shown in appendix. Essential outputs of the analysis are summarized in Table 4. Because the test specimens were cut into single-tee members, the values in the table are one-half of the

moments and shears determined for the baseline DT. Stresses reported in the table are the maximum tensile stresses which occur at mid-span. Composite action between the precast member and deck was considered when calculating stresses due to superimposed dead load and live load. The test specimens and the test set-up were designed (presented in the next chapter) such that the service level tensile stresses and service level shear force occurred at approximately the same applied load in the tests.

Table 4. Structural demands on baseline beam (for one stem of the baseline DT)

Condition	Moment (kip-ft)		Shear at 5ft (kip)		Concrete tensile stress (psi)	
	NWC	LWC	NWC	LWC	NWC	LWC
Service	323	305	17.9	16.9	966	757
Ultimate	430	410	23.9	22.7	NA	NA

IV.   IMPACT OF DT WEIGHT REDUCTION

Obvious questions of this research program include: Do foam voids allow two DT members to be transported on one truck? What is the degree of weight-loss due to the foam voids? This section provides context and answers for these questions.

Many factors influence the possibility of two-at-a-time trucking. The self-weight of the DT is a primary factor. Self-weight is a function of the concrete unit weight, the span length and cross-section, and the volume of the foam void (in any). Other factors include the weight of the truck and trailer, and the gross vehicular weight (GVW) limit for the highway system. GVW limit in the United States is typically 80 kips.

Figure 10 presents different combinations of foam void and concrete unit weight that (dis)allow two-at-a-time trucking. The figure is only based on weight limits and does not imply that any particular combination of concrete weight and foam void width is structural viability. The remainder of this thesis focuses on structural viability. Using the figure, a designer can select a unit weight, foam width, and a cross-section size that are likely to allow two FVDT to be transported on the same truck.

Figure 10 is based on a combined truck and trailer weight of 26 kip; this value was chosen based on the industry survey. The figure assumes that the foam void is 12 in. deep in each stem and that the member length is 60 ft. The graph is for field-topped members only. These assumptions must be checked when applying the figure.
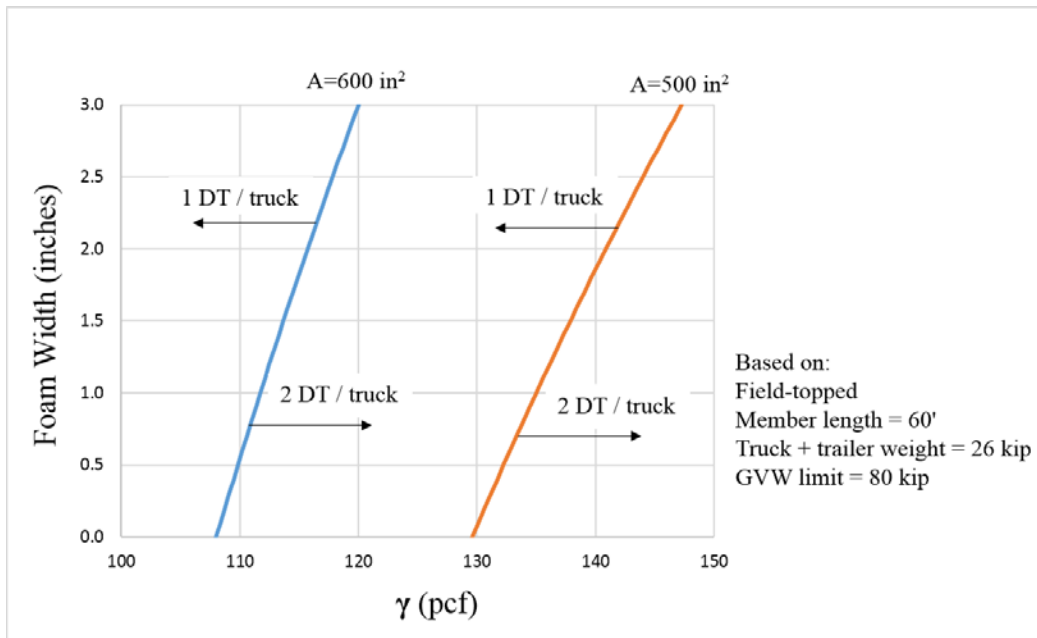
Figure 10. Variation of unit weight with foam thickness to meet GVW limits

The 28 in. deep test specimens discussed in the remainder of the thesis had cross-sectional area of 596 in² and concrete unit weights of 126 and 145 pcf. From Figure 10 it can be observed that the 126 pcf specimens would require a foam width larger than 3 in. to qualify for two-at-a-time trucking. Because the foam void concept has not previously been tested, the experimental program took a conservative approach using 1 inch and 2 inch wide foam voids. The test program focused on finding foam void details that were structurally viable while also achieving a degree of weight reduction. Thus, the program identified an amount of foam void that is structurally viable, but it did not find the upper limit for structurally viable void size.

The void widths used in the test program were 12 in. deep and either 1 in. or 2 in. wide. Relative to solid 28" deep DTs, these widths correspond to a 4% and 8% weight reduction for the 1 in. and 2in. wide voids, respectively. Although this level of weight

reduction does not satisfy the requirements of two-at-a-time trucking for the assumptions in Figure 10, it may be sufficient in other circumstances such as shallower members, shorter members, or members with lighter-weight concretes. Even when two-at-a-time trucking is not permissible, reduced weight still has the benefit of reducing overall structural demands.

V. EXPERIMENTAL PROGRAM- SPECIMENS AND SETUP

Overview

An experimental program was conducted to study flexural and shear capacity of DT members with foam voids. For efficiency in testing, each "specimen" in the study was a single-tee member. Two FVDT members were cut lengthwise into four single-tee specimens. This chapter describes design, fabrication, and testing of the specimens and provides interpretation of the test results. Specific objectives of testing included:

- Evaluate experimental flexural capacity of FVDT relative to calculated nominal capacity;
- Evaluate experimental shear capacity of FVDT relative to factored shear force in the baseline beam; and
- Evaluate cracking (if any) at the end of the foam void.

Specimen Design and Construction

Specimens were created from two 35' long 12DT28 members. One of the members was cast with normal weight concrete (145 pcf) and the other with semi-light weight concrete (126 pcf). One stem of each DT member had a 1 in.-thick foam board, and the other stem had a 2 in.-thick foam board. Each specimen was given a unique label based on the concrete unit-weight and width of foam board (Figure 11).
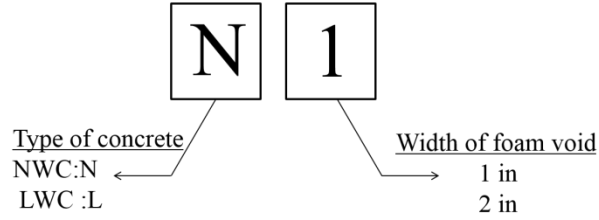
Figure 11. Test specimen labeling

The concrete unit-weights were chosen in consultation with the specimen fabricator; mix designs were typical of those used for production members. The foam width and reinforcement were also selected in consultation with the fabricator.

Cross section, elevations, prestressing, and reinforcement details of the specimens are shown in Figure 12 and Figure 13. The edges (5 ft. from the ends), length (25 ft.), and depth (12 in.) of the foam boards were the same in all four specimens (Figure 13).
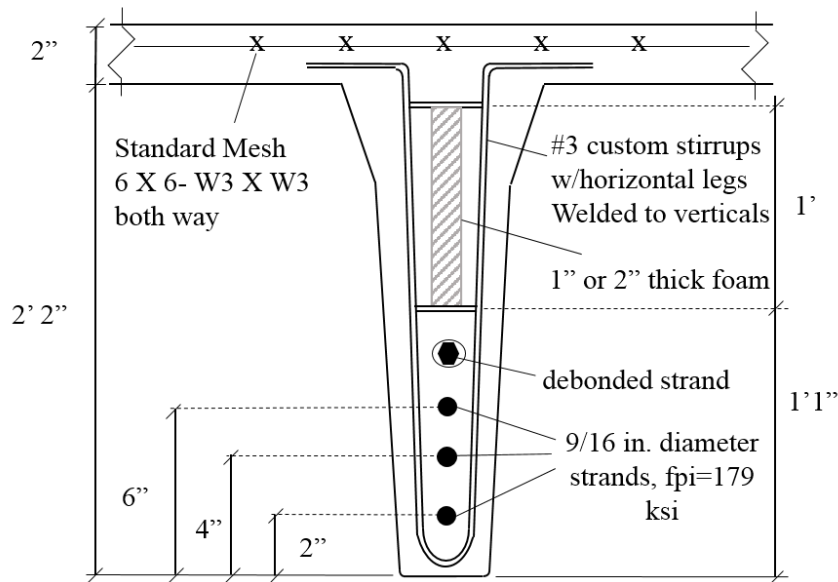
Figure 12. Specimen cross section
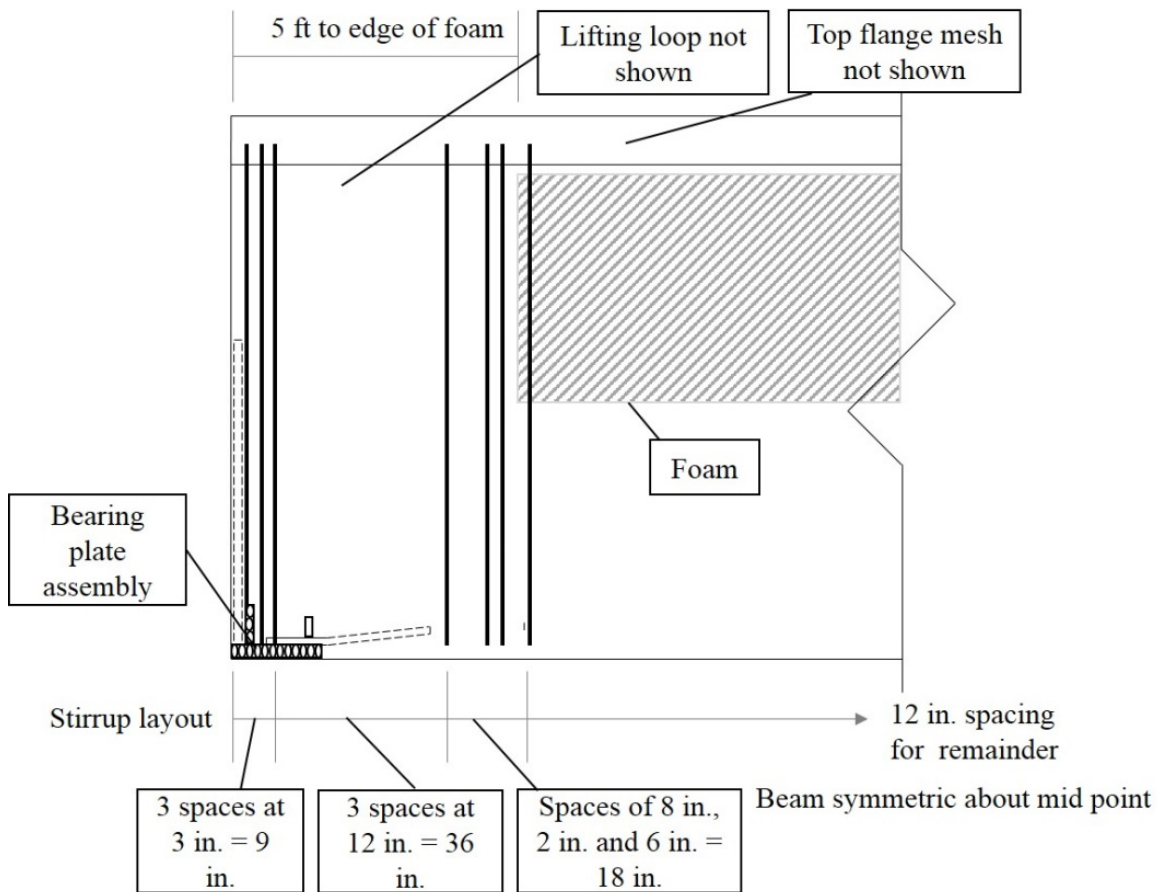
Figure 13. Specimen vertical reinforcement

The test specimens were fabricated in the same bed as production members for a building project, and the strand pattern (Figure 12) was based on the production members. As the test specimens had a shorter span than that of the production members, stresses in the specimens were controlled by debonding the top-most strand. For safety purposes, a 3 ft. segment of the top-most strand was bonded at mid-span.

Transverse reinforcement in the specimens were custom-made #3 stirrups (Figure 14), which included an opening for holding the foam board. The horizontal pieces in the stirrups were welded to the vertical legs to form the opening. The stirrups were anchored

19

down by the strands, and the foam was anchored down by the stirrups. Concrete and

reinforcement material properties are listed in Table 5 and mix designs for the normal

weight concrete and light weight concrete are shown in Table 6 and Table 7. The

members were fabricated in fall 2015. Photos of construction are shown in Figure 15 and

Figure 16. The specimens were designed by Srimaruthi Jonnalagadda, who also

documented the fabrication process.

Figure 14. Custom #3 stirrup used as transverse reinforcement

Table 5. Material properties of concrete and reinforcement

Material	Properties
Semi-light weight concrete	28 day compressive strength: 7810 psi 401 day compressive strength: 11310 psi 441 day compressive strength: 10360 psi Unit weight: 126 pcf *Note: The same concrete was used for all LWC beams. Load tests were conducted between days 401 and 441.*
Normal weight concrete	28 day compressive strength: 7270 psi 464 day compressive strength: 9610 psi 576 day compressive strength: 10790 psi Unit weight: 145 pcf *Note: The same concrete was used for all NWC beams. Load tests were conducted between days 464 and 576.*
#3 reinforcing bars	ASTM 615M-14 Grade 420/60 Yield Strength: 77.4 ksi (534 MPa) Tensile strength: 107 ksi (738 MPa) *Note: properties based on rebar supplier documentation*
9/16 in. diameter strands	Type: Low- Relaxation Strands Tensile Strength: 270 ksi

Table 6. Mix design of normal weight concrete

Item	Batch quantity	Units
Type II/III cement	565	lb/cy
Class "F" fly ash	140	lb/cy
C-33 sand	1247	lb/cy
57 stone granite	1534	lb/cy
Water	281	lb/cy
Air admixture		
HRWR admixture		
Inhibitor admixture		
Air (6%)		

Table 7. Mix design of light weight concrete

Item	Batch quantity	Units
Type II/III cement	700	lbs/cy
Class "F" fly ash	150	lb/cy
C-33 sand	1146	lb/cy
3/8" granite	377	lb/cy
1/2 Stalite	656	lb/cy
Water	279	lb/cy
Air admixture		
HRWR admixture		
Inhibitor admixture		
Air (6%)		

Figure 15. FVDT prior to casting

Figure 16. Concrete placement in stem

Test Set-up

The specimens, boundary conditions, and load locations were designed such that the shear forces and flexural-tension stresses in the specimens mimicked those of the baseline beam. Accordingly, a simple-span four-point bending configuration was selected (Figure 17). At an experimental load of approximately 28 kip (total for both load points) shear force in the specimens at the edge of the foam void was approximately equal to the service-level shear force in the baseline beam at the same location. Also at a load of 28 kip, the flexural-tension stress at mid-span of the specimens were approximately 15% less than the service-level stress of the baseline beam. The "service load" referred to in this thesis corresponds to a total applied load of 28 kip. These comparisons between the test specimens and baseline beam are based on the normal-weight concrete specimens.
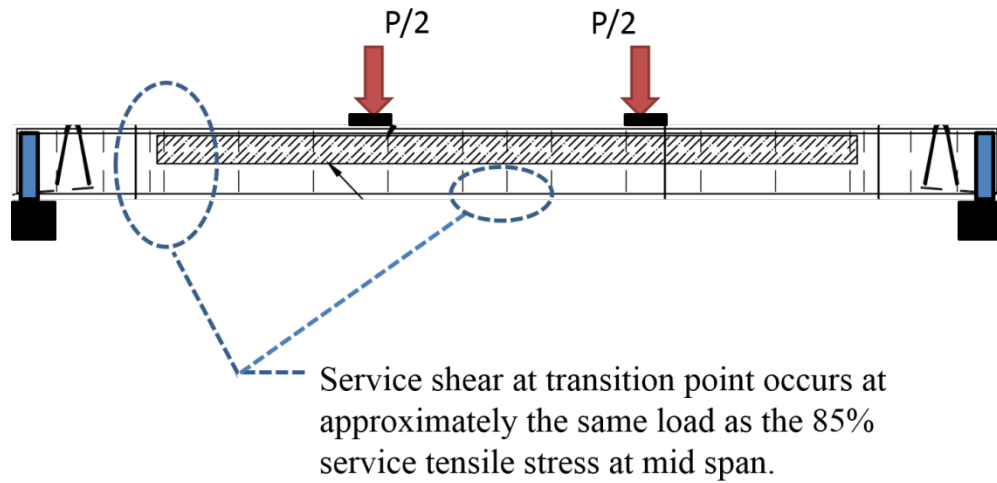
Figure 17. Support and load configuration for FVDT test specimens. Locations of interest for shear force and tensile stress are also shown

The test set-up included features to ensure stability of the single-tee specimens during testing. This was done by using a steel "saddle" support (Figure 19) at both ends to restrain rotation along the long axis of the specimen. The saddles were effective and no rotation or specimen instability was observed during testing.

Corners of flanges were cut as shown in Figure 18 in all the specimens to facilitate bringing the specimens into the lab. Cuts were only made at the ends of the beam and it is reasoned that thee cuts have negligible impact on strength of the beam.

Figure 18. Flange cut-off location at the ends of the specimen

Load was applied quasi-statically using a hydraulic jack at a rate of approximately

250 pounds per second. A steel I-beam was used to spread load from the jack to the

specimen (Figure 20). Rubber bearing pads were used at all support and load points.

Figure 19: Specimen braced by "saddle" at each support

Figure 20. I-beam used for spreading load from jack to specimen

Displacement, strain, and force were monitored and logged using a computer data acquisition system. Strain gage locations are shown in Figure 21 and string potentiometer locations are shown in Figure 22. String potentiometers were used to record vertical displacement at mid-span of the specimens, where two were attached to stem and two were attached to flange. Six strain gauges monitored concrete surface strain, two at the edges of the foam voids, two on the bottom of the specimen below the load points, and two on top of the flange at mid-span. The applied load was recorded using a pressure gage, which was calibrated immediately prior to conducting the tests, and installed in the hydraulic line supplying the jack. Area of the jack was 20.65 in^2, therefore the applied force was calculated by multiplying the gage pressure by the jack area.
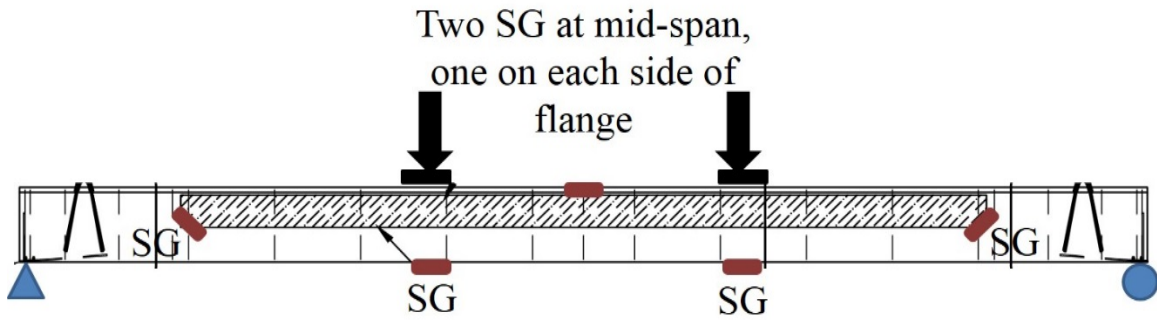
Figure 21: Strain gauge (SG) locations
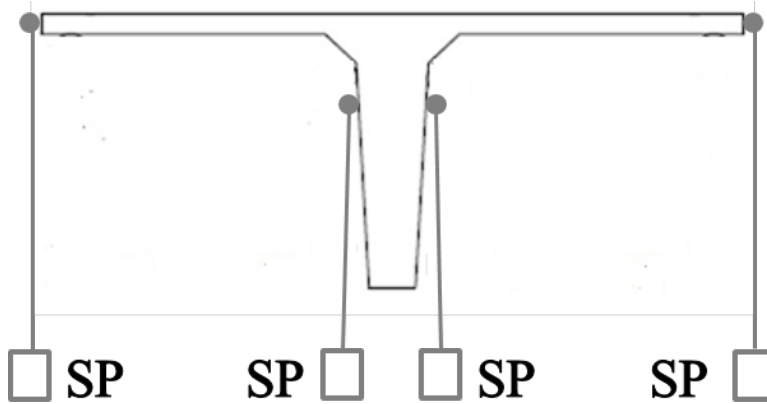
Figure 22: String pots (SP) locations. All SPs attached at mid-span

Specimens were loaded in seven different stages, in the following order:

1. Quasi-static load to 50 % of service load

2. Cyclic load (non-dynamic) between 20% to 50% of service load

3. Quasi-static load to 100% of service load

4. Cyclic load (non-dynamic) between 20% to 100% of service load

5. Sustain load test at 100% service for 24-hours (specimen L2 only)

6. Quasi-static load to flexural capacity

7. Quasi-static load to shear capacity

With the exception of stage 5 (more on this later), the tests were not based on any standard code provisions. The test type and test sequence were selected to gradually introduce load so that behavior could be evaluated under increasing levels of stress.

Details of the test geometry are presented in Figure 23 and Table 8. The geometry of the test setup changed slightly during testing because a new spreader beam was introduced after the test program was underway. The original spreader beam did not have sufficient capacity to support the flexural load tests, particularly during shear testing. Changes in geometry from the spreader beams were minor. The only significant change in geometry during the test program was span length used during the shear tests (stage 7). For these tests, the supports were moved to the edges of the foam voids to ensure that the maximum shear force was applied through the foam void section. For all other tests, the supports were located at the ends of the specimens.

In cyclic load tests (stages 2 and 4) load was applied for 100 cycles. Load cycles were referenced to the service load. Data from the pressure gauge, strain gauges, and string potentiometers were acquired only for the first five and last five cycles. The 24 hour sustained load test (stage 5) was conducted following the ACI 318-14, chapter 27[11].

The specimens were fabricated in fall 2015 and were brought the Clemson lab in fall 2016 for testing. The gap between fabrication and testing was due to construction of the strong floor at the Clemson lab. Testing began in October 2016 and ended in October 2017. The schedule of all the tests is shown in Table 9.
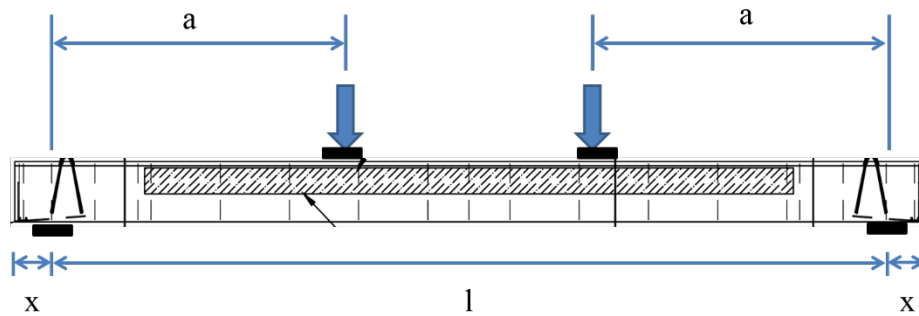
Figure 23. Dimensions to centerline of supports and to the end of specimen

Table 8. Test set up parameters

Stage Number	Stage Description	Geometry (ft)		
		a	L	X
1	50 % service load test	12 (typ) 11.9 (N2)	34	0.5
2	20 % - 50 % cyclic load test	12 (typ) 11.9 (N2)	34	0.5
3	100 % service load test	12 (typ) 11.9 (N2)	34	0.5
4	20 % - 100 % cyclic load test	12 (typ) 11.9 (N2)	34	0.5
5	Sustained load test (only for L2)	12	34	0.5
6	Flexural load test	12 (typ) 11.9 (N2)	34	0.5
7	Shear test	7 (L1 & L2) 5.4 (N1 & N2)	25 (L1 & L2) 22(N1 & N2)	5 (L1 & L2) 6.5 (N1 & N2)
*Unless Noted Otherwise, stages and geometry are typical for all specimens.				

Table 9. Tests schedule

Schedule of tests					
Stage Number	**Stage Description**	**Number of days after casting***			
		L1	**L2**	**N1**	**N2**
1	50 % Service Load	380	410	494	653
2	20% to 50% cyclic load	380	410	494	653
3	100% Service Load	387	420	500	688
4	20% to 100% cyclic load	387	420	500	688
5	Sustained Load Test	------	439	------	------
6	Flexural Load Test	389	444	507	694
7	Shear Test	396	472	569	729
*Specimens were cast on 10/06/2015					

VI. TEST RESULTS

Data from testing are typically reported in terms of moment and mid-span displacement. Unless noted otherwise, the report displacement is always the average displacement of the four spring potentiometers at mid-span. Displacement values do not include self-weight displacements or camber. Moments are reported as the maximum moment due to the applied loads and, except in a few cases which are clearly labeled, do not include moment from self-weight. Similarly, strain data are only the strain due to applied loads. Positive denotes tensile strain.

Stage 1: 50% service

The beams were loaded up to 15 kips in stage 1 to verify stability and adequacy of the test set-up and to evaluate the performance of the FVDT specimens at low load levels. The behavior of all specimens was similar for stage 1.The moment-displacement behavior was linear-elastic for all the specimens and no visible cracks were observed during this test stage. Strain data were linear-elastic, which confirmed the absence of cracking. Specimens displaced 0.2 to 0.25 inches in stage 1. Moment-strain plots for stage 1 are shown in appendix. Based on specimen stability and performance during stage 1, a decision was made to proceed with the subsequent stages.

Stage 2: 100 Cycles between 20% and 50% service load

Parking garage DTs are subjected to millions of cycles of loading. In Stage 2, specimens were tested for 100 cycles between 20% and 50% of the service load. Admittedly, 100 cycles do not approach the condition of DT members in a parking

31

garages and performance of the specimens after 100 cycles does not suggest that the specimens would perform similarly after millions of cycles. However, testing for 100 cycles was still deemed valuable because any issues observed during the first 100 cycles would provide evidence to reject the foam-void concept.

Strain data from edges of foam and under point loads are shown in Figure 24 and Figure 25. These data are from the last five load cycles for specimen L1 and are representative of all specimens. Cracking was not observed either visually or in the strain data. If cracking had occurred it would be reflected in the data as abrupt and extreme changes in strain. Strain data in the tests was effectively linear-elastic and did not have abrupt changes. It is also encouraging that cracks were not visually observed at the edges of the foam during this stage. Also, as expected, flexural cracking did not occur during stage 2.

Due an experimental error in stage 2, the peak load on L1 reached 65% of the service load during one of the cycles. This did not affect in cracking at the edges of the foam, but did result in flexural cracking and consequently reduced stiffness for L1 in state 3.
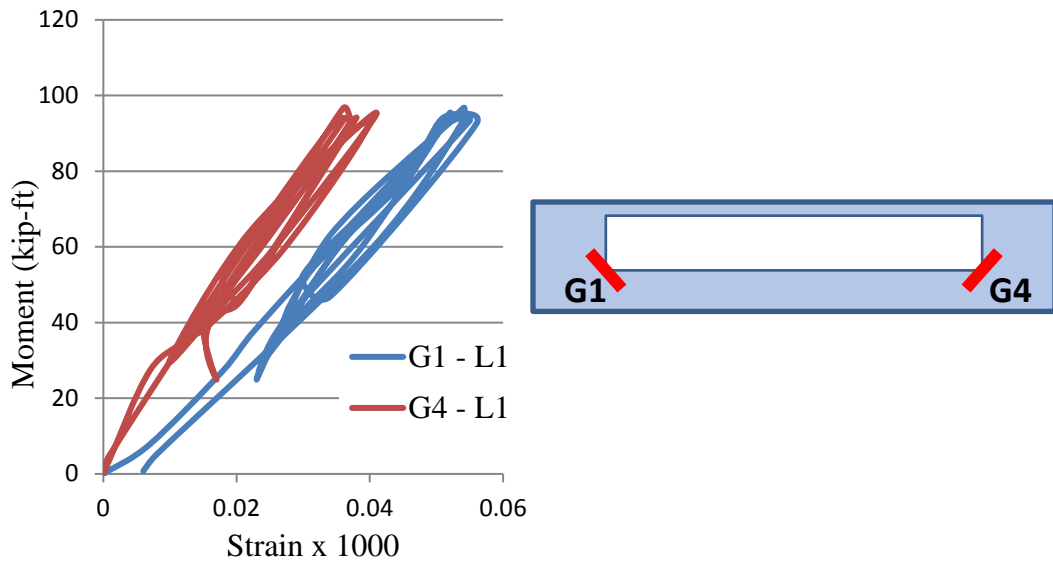
Figure 24. Moment-strain response at edges of the foam for last five cycles during test
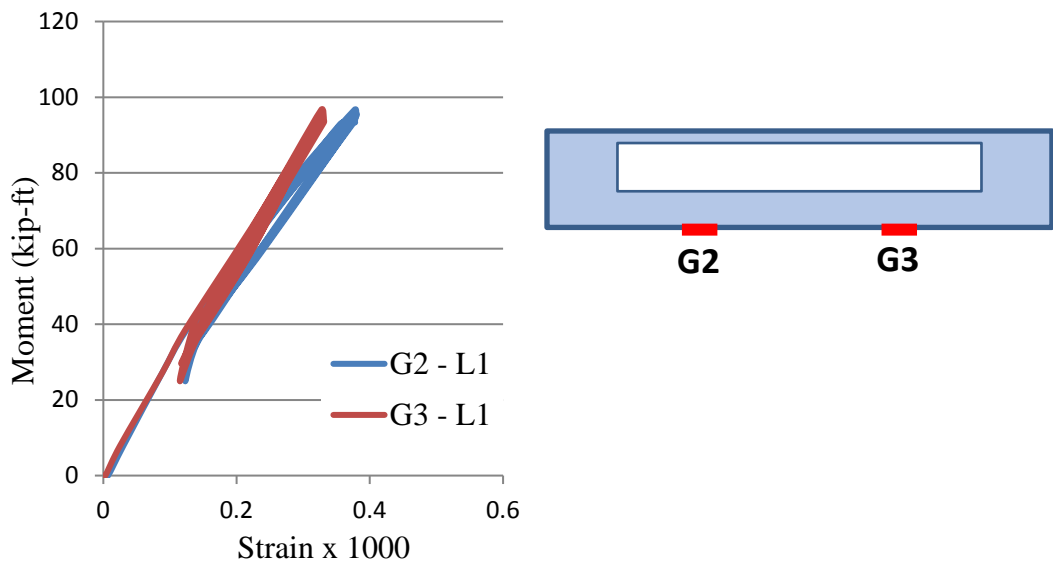
stage 2

Figure 25. Moment-strain response under point loads for last five cycles during test stage

2

Stage 3: Static test to 100% service load

The beams were loaded up to 100% service load (i.e. 28 kips) to evaluate service-level performance. Similar behavior was observed in all the specimens. Based on prior stress analysis of the specimens, flexural cracks were expected. Flexural cracking was visually observed in all specimens between the load points. Moment-strain data for the gauges under the point loads are plotted in Figure 26. Nonlinear strain response at higher moments in some specimens also indicates the occurrence of cracking. Cracking was more obvious in the L1 strain data and less obvious in strain data from the other specimens.
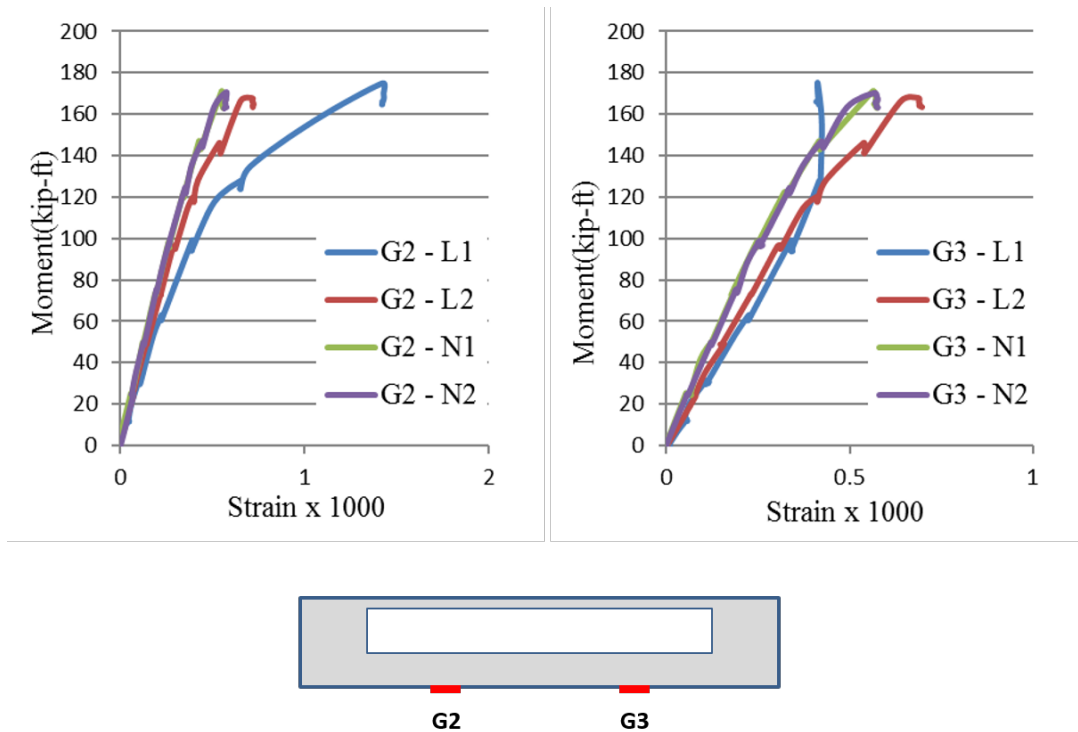
Figure 26. Moment-strain plot for gauges under the point loads in test stage 3

Moment-displacement plot for all the specimens is shown in Figure 27. The displacement was higher in case of L1 because it had undergone flexural cracking in stage 2; the other specimens had not cracked during stage 2. Flexural cracks in L1 reopened at an applied moment near 120kip-ft during stage 3. Near the end of stage 3, the normal-weight concrete specimens showed greater stiffness than the light-weight specimens.
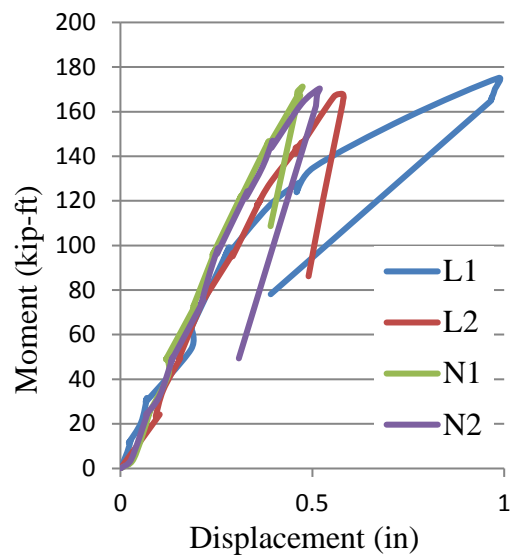
Figure 27. Moment-displacement plot for all the specimens in test stage 3

Strain data (Figure 28) show linear-elastic response for all gages except G1 on specimen N1. This indicates that cracking did not occur during stage 3. In addition to strain data, visual observations also confirm that cracking did not occur at the edges of the foam during this stage.

The moment-strain data for specimen N1 at one end of the foam region shows nonlinear behavior (Figure 28 left). This may be due to cracking but the nonlinear strain

response was not observed in flexural load test (stage 6) results at that location. No cracks were visually observed at the gage location. Thus, while the nonlinear behavior in N1 (gage G1) is noted, observations and data from other stages suggest that cracking did not occur at the edge of the foam.
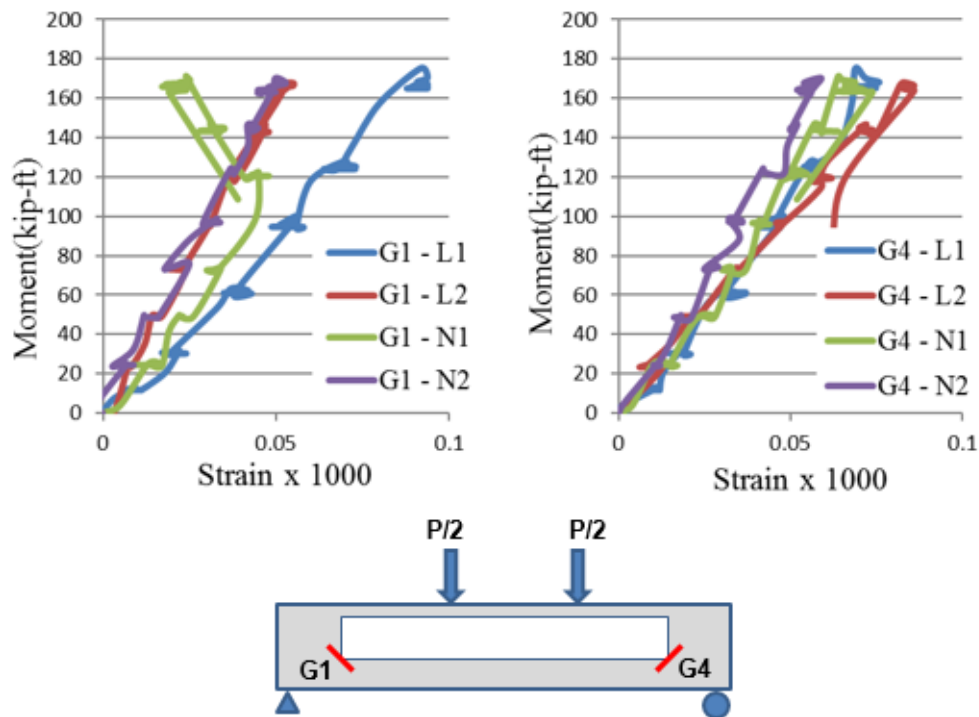
Figure 28. Moment-strain response at edges of the foam during service load tests

Strain data from gauges at the edge of the foam (e.g. Figure 28) has more noise than strain from other gauges (e.g. Figure 26). This is primarily due to the relatively low magnitude of strains measured at the edges of the foam and due to the sensitivity of the gauges at low strain levels. The "clusters" of strain data occurring at intervals along the data are due to pauses in loading.

Stage 4: 50% to 100% service

The same procedures and approach were taken for this stage as was described for stage 2. The only difference was that the load level ranged from 50% to 100% service load.

Strain data at edge of foam for last five cycles in the specimen L1 are shown in Figure 29; data from other specimens are shown in the appendix. Based on strain data and visual inspection, no cracking occurred at edges of foam. In case of the specimen L1, the strain data at the edges of foam shows that there was approximately 20 micro strain of residual strain after testing. Residual strains at the edges of the foam were not observed in stage 4 data from the other specimens (L2, N1, and N2). While the residual strain is noted in the data for specimen L1, no conclusions are reached regarding this observation. If the residual strain was indicative of concrete damage, then cracking would be expected during the subsequent flexural load test (stage 6). No cracking at this location was observed visually or from strain data in the flexural test (stage 6) of L1.
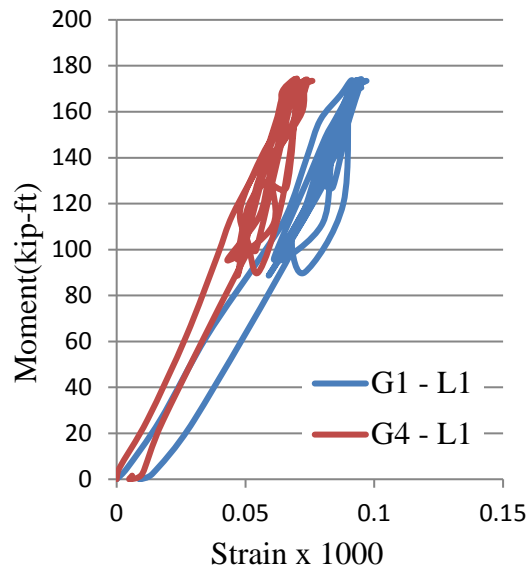
Figure 29. Moment-strain at edges of the foam for the last five cycles

Stage 5: 24 hour sustained load test

This stage was conducted only for specimen L2. The test procedures followed

ACI 318-14 Chap. 27 [11]. The total applied load was 40 kip, which produced

approximately the same flexural stresses in the specimen as the load-level prescribed by

equation 27.4.2.2a in ACI 318 would produce in the baseline beam. Shear force in the

specimen at this load level was approximately 32% higher than the shear force in the

baseline beam at the ACI 318 specified load. The applied load in stage 5 was greater

than loads in stages 1 through 4.

The ACI 318 Chapter 27 test procedure provides a means of assessing structures

capacity of existing members. Flexure capacity for the sustained load is assessed by

considering total and residual displacements. The total displacement due to the loading at

the end of this test was 2.7 inches, and the residual displacement after load was removed

was 0.19 inches. Results are shown in Table 10 and comparisons to the ACI requirements (27.4.5.5b) are shown in Table 11. To pass the requirements of ACI 318 Chapter 27, one of two conditions must be satisfied. First, the total displacement must be less than the value given by $l_t^2/20000h$, where l_t is the span length and h is the member height. Second, the residual displacement (Δ_r) must be less than ¼ of the total displacement (Δ_1) at the end of the sustained load test. The specimen satisfied the second criteria and was deemed as passing. Because the residual displacement was less than ¼ of the total displacement, it was concluded that the specimen could likely have supported greater displacements before reaching flexural capacity.

Table 10. Results of 24 hr sustained load test

Load (kip)	Deflection (in)
0	0
8	0.13
16	0.31
24	0.56
32	1
40(Initial)	2.38
40(Final)	2.69
0	0.19
Total Displacement, Δ1=	2.69
Residual Displacement, Δr=	0.19

Table 11. ACI conditions for 24 hr sustained load test

ACI Conditions:					
1)	$\Delta_1 \leq l_t^2/20000h$ l_t = 34 ft, h = 28 in	Δ_1	>	$l_t^2/20000h$	Not
		2.69 in.		0.30 in.	Satisfied
2)	$\Delta_r \leq \Delta_1/4$	Δ_r	<	$\Delta_1/4$	Satisfied
		0.19 in.		0.67 in.	

Stage 6: Flexural load test

Load-displacement behavior during the flexural tests for all specimens is shown in Figure 30. The figure also shows the moments associated with service level flexural stresses and nominal flexural capacity. Comparisons with nominal flexural capacity will be made in the next section.
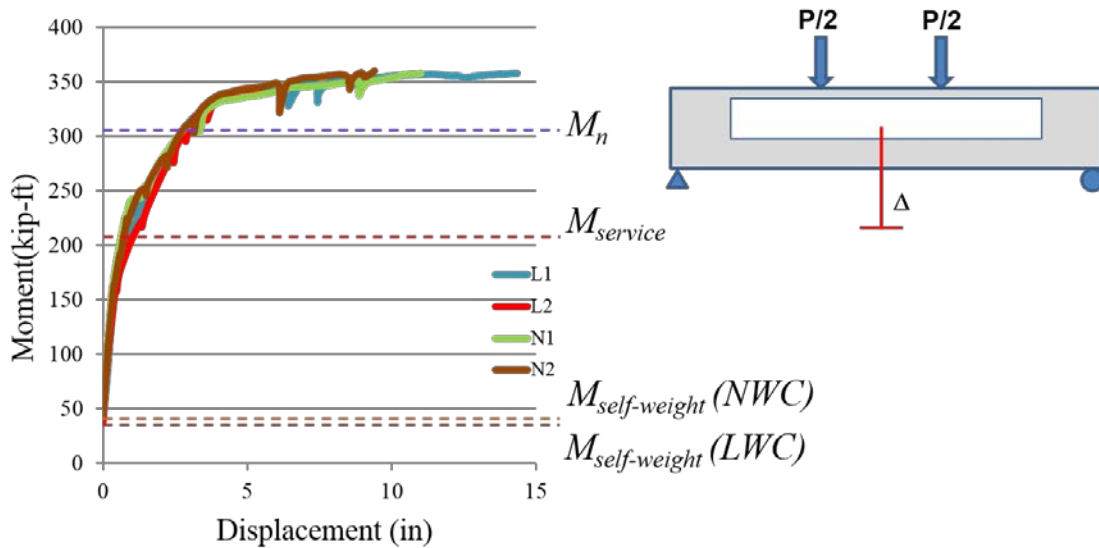
Figure 30. Moment-displacement response during flexural tests

Load-displacement behavior was similar for all specimens during the flexural tests. Response was initially linear-elastic. Stiffness decreased as flexural cracking opened at a load of approximately ~19 kip (~120 kip-ft of moment). These cracks had already formed during service load testing, so opening of the cracks at ~19 kip (~120 kip-ft of moment) corresponded to decompression of the prestress.

New cracks formed and existing cracks extended (Figure 31) as load was increased beyond the previous peak of 28 kip (175 kip-ft of moment from the service

load tests). As the force approached 50 kip (313 kip-ft of moment), stiffness was

effectively gone and the displacement was imposed without significant increase in load.

Testing continued until the jack reached its maximum stroke length. Because of changes

in the spacers and I-beams placed between the jack and specimen, the maximum

displacement achieved during testing was different for each specimen. Thus, maximum

displacement was a function of test set-up and is not used for comparison of specimens.

Figure 31. Widening of the cracks and formation of new cracks during flexural load test

Crushing of the top flange was not observed in any of the specimens during the

flexural load tests. It is likely that the specimens could have supported additional

displacement prior to crushing of the flange; however, it is not likely that the peak load

would not have increased significantly. Residual displacement of approximately 3 in.

(specimen L2) to 10 in. (specimen N1) was observed in the specimens after the load was removed.

Each specimen's behavior was ductile at loads near the peak experimental load. However, relative ductility of specimens cannot be compared using the available data. As previously mentioned, testing was terminated when the hydraulic jack reached the maximum stroke; based on differences (height of spreader beam and spacers between the specimen and jack) in test setups, the available stroke length was different for each test. Thus, the apparent differences in ductility are a function of testing limitations and not a function of the specimens.

Strain gages G1 and G4 were placed at angle on the concrete surface near the foam ends (Figure 32) to monitor for cracking. This location is of interest because of the abrupt change in cross section due to termination of the foam. The rational for placing the gages at an angle were to approximately align with the direction of the principal tensile stresses. Load-strain response of these gages was effectively linear-elastic throughout the flexural load tests (Figure 32), suggesting that cracks did not form at this location. Visual inspection during testing also confirmed that cracks did not form in the concrete adjacent to the ends of the foam. Thus, it is considered unlikely that shear cracks would form at this location in FVDT parking garage members having similar detailing and material properties as the test specimens.
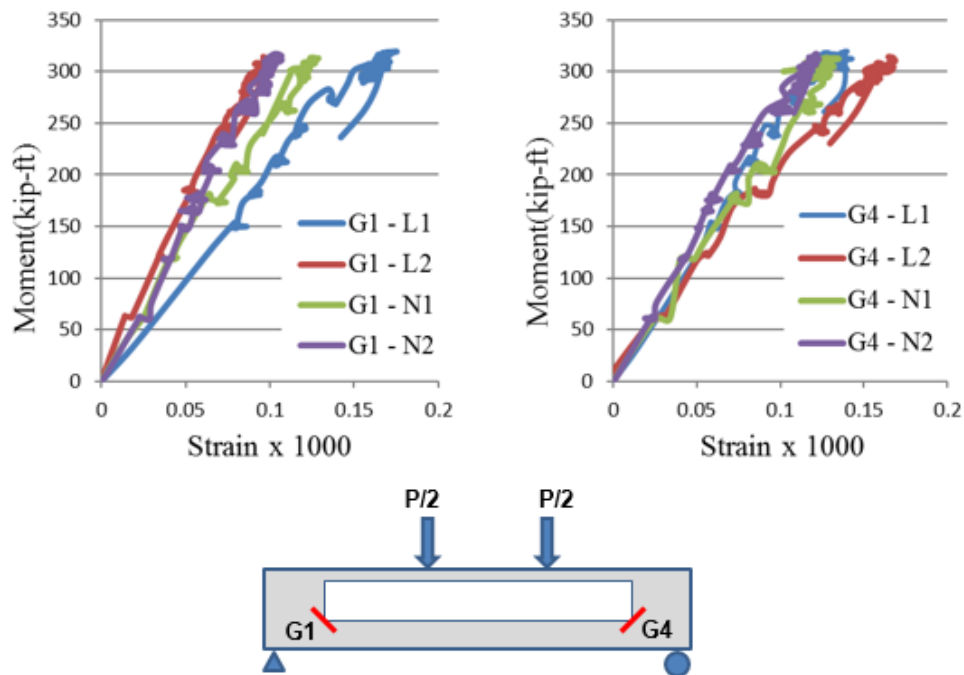
Figure 32. Moment-strain response at edges of the foam during flexural load tests

Figure 33 shows the cracks in the web at the mid-span of specimens after approaching to the ultimate load. Figure 34 shows the propagation of cracks in specimen L1 throughout the loading stages. This pattern of cracking was similar for all specimens. The majority of the cracks in the stems occurred within the middle 20 ft of the specimens. Flexural cracks originated during the service load testing and then expanded and developed further from the load points during the flexural load test.

Figure 33: Crack pattern around mid-span of all the beams during flexural load test

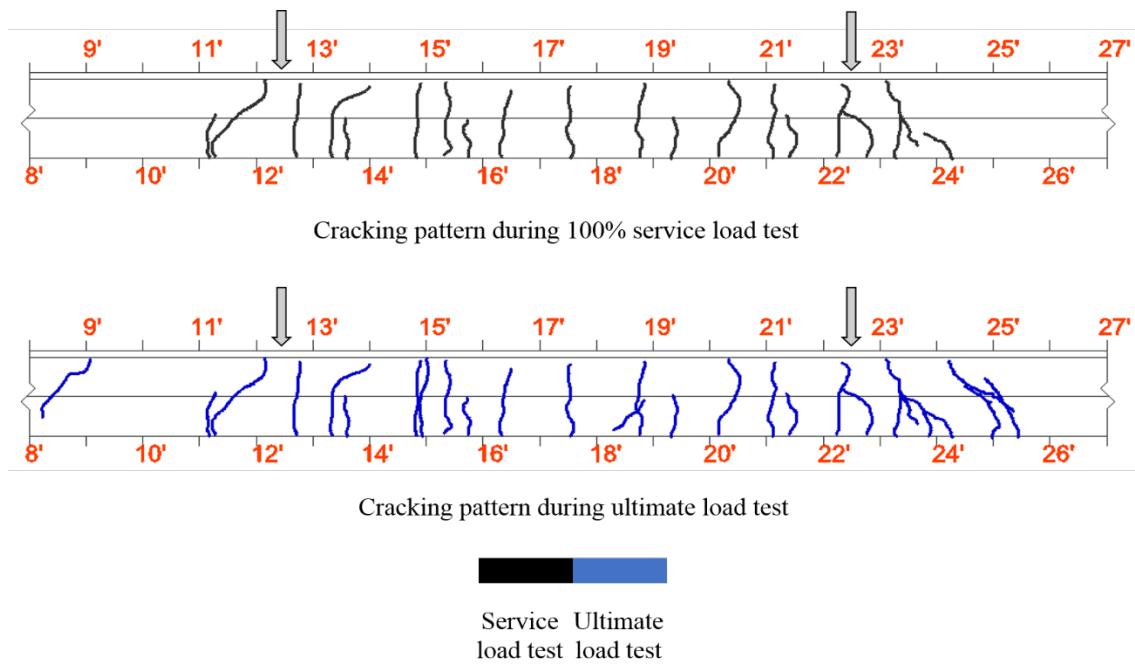Cracking pattern during 100% service load test

Cracking pattern during ultimate load test

Service Ultimate
load test load test

Figure 34: L-1 Cracking Pattern

Stage 7: Shear load test

In the final stage, the specimens were tested for shear capacity. The supports were moved inwards by 5 to 6 ft on both ends so that the maximum shear force was carried through the foam void section. Displacement data were collected using string potentiometers; however, these data are not insightful as the specimens had already cracked by this stage and there was a residual set in them. The main insight behind this test stage was to find the experimental shear capacity.

Failure behavior was distinct for different specimens. Specimen L1 failed in flexure due to a strand rupture (shown in Figure 35) below one of the load points. Specimen L2 did not fail completely as it was not possible to load it further after the stroke length of the cylinder reached its maximum limit. Specimens N1 and N2 failed in flexural-shear (shown in Figure 36 and Figure 37). It can be observed from figures that in case of N1, the crack crossed one stirrup before reaching the flange and in N2, the failure resulted from the crack which reached the flange straight from the web without crossing any stirrup. The critical cracks (those associated with shear failure) in N1 and N2 had occurred during flexural testing. For N2 the failure occurred due to shear failure of the compression zone. For N1 the failure was a more classical flexural-shear mechanism. The peak applied shear force, failure mode, and other observations of each specimen are summarized in Table 12.

Figure 35. Specimen L1 at location of strand rupture

The upper-most strand in the photo was the debonded strand which was cut after the test program was finished.

Figure 36. Flexure-shear failure in the specimen N1

Figure 37. Compression zone shear failure in the specimen N2

It may be questioned that a virgin specimen should be tested to determine experimental shear capacity. By the time that the beams were tested in shear in stage 7 they had been subjected to flexural cracking from the earlier stages. It is reasoned that the shear strength of damaged (pre-loaded) beams should be the same or lower than if the shear tests were conducted on a virgin beam. It is considered unlikely that the shear strength of an undamaged beam would be less than the shear strength of the damaged test specimens.

Table 12. Shear test results

Shear test results of all the specimens			
Specimens	**Failure Mode**	**Peak Shear (kip)**	**Notes**
L1	Flexural (strand rupture)	46.7	Strand rupture below load point and resulted in sudden collapse
L2	Not failed	58.9	Terminated due to reaching maximum stroke length of jack
N1	Shear	47.5	Flexural-shear failure below the load point
N2	Shear	59.1	Flexural-shear failure below the load point

VII.   ASSESSMENT OF EXPERIMENTAL OBJECTIVES

Comparison with nominal flexural capacity

The first objective was to evaluate experimental flexural capacity of FVDT specimens relative to their calculated nominal capacity. Flexural capacity was calculated using the strain compatibility approach. Calculations (shown in appendix) used the constitutive model for strands from the PCI Design Handbook [9]. Based on material tests, average concrete compressive strength used in the flexural calculations was taken to be 9380 psi for NWC and 9880 psi for LWC. The presence of foam did not impact the calculations because the theoretical compression block was within the flange at nominal capacity.

The experimental capacities were reasonably close calculated nominal flexural capacities. The experimental moments exceeded the calculated nominal flexural capacities by 15% to 17% (Table 13). On average, the specimens supported experimental moments that were 16% larger than their nominal flexural capacities.

Table 13. Comparison of experimental and nominal moments

Specimen	Max moment due to self-weight (kip-ft)	Max moment due to applied load (kip-ft)	Total experimental moment, M_{exp} (kip-ft)	Nominal flexural capacity, M_n (kip-ft)	Strength ratio, M_{exp}/M_n
L1	38.3	320	358.3	305.5	1.17
L2	36.7	314.4	351.1	305.5	1.15
N1	44.1	314.4	358.5	305.3	1.17
N2	42.3	319.4	361.6	305.3	1.17
				Average	1.17

The experimental moment was compared with the nominal capacity of the specimens rather than that compared with the nominal capacity of the baseline beam. This is due to the fact that the cross-section and prestressing were different than in the test specimens than the baseline. Although the experimental and nominal capacities of the specimens cannot be compared directly with the baseline beam, the level of agreement between the experimental moment of the specimens and their nominal capacity suggests that the same calculation approach would be appropriate for the baseline beam. For the first objective, it is concluded that the nominal capacity calculations were conservative but sufficiently accurate (within 15%) for FVDT, and the strain compatibility-based flexural calculations are accurate for FVDT members.

Comparison with factored shear of baseline beam

For the second objective, the experimental shear was compared with the factored design shear force in the baseline beam. Recall that the shear demand in the baseline beam is 28.7 kip (NWC) and 27.3 kip (LWC) (Table 12). These shear forces are located 5 ft from the ends of the baseline, this is the location wherein the foam void started in the specimens.

Maximum experimental shear forces and factored shear demand in baseline beam are compared shown the Figure 38. Because of the support set-up for the shear tests, the maximum experimental shear force crossed the foam-void section of the specimens. In most cases, the maximum experimental shear force corresponded with shear failure; however in the case of L2 the maximum shear did not result in failure (see discussion of

test stage 7). Figure 38 also shows the contribution of the reinforcement to the nominal shear (V_s) capacity of the specimens. This quantity was calculated using ACI 318 equation 22.5.10.5.3 [11]. The concrete contribution was not consdiered in the calculations because the shear area was interupted by the foam voids. As such, it was considered conservative to ignore the concrete contribution.

Two points are made regarding Figure 38 . First, the experimental shear forces were significantly (at least 66 %) more than the factored shear demand in the baseline beam. This suggests that the beams with foam voids may be suitable for carrying shear forces in parking garages. Second, the experimental capacity was significantly more than the steel contribution to nominal shear capacity. From this result it is concluded that the concrete, inspite of the foam, was a significant contirbutor to shear capacity. This may be attributed to the relatively high concrete strength, which was approximately 10 ksi at the time of testing. It is suggested that lower concrete strength be considered in any future tests.

The test specimens did not have a topping slab which would be present in the baseline beam. The presence of topping would likely have increased the shear capcity of the specimens; however, the specimens exceeded the baseline beam's shear demand even without the topping. This further confirms that FVDT specimens were more than sufficient for carrying parking garage shear loads.
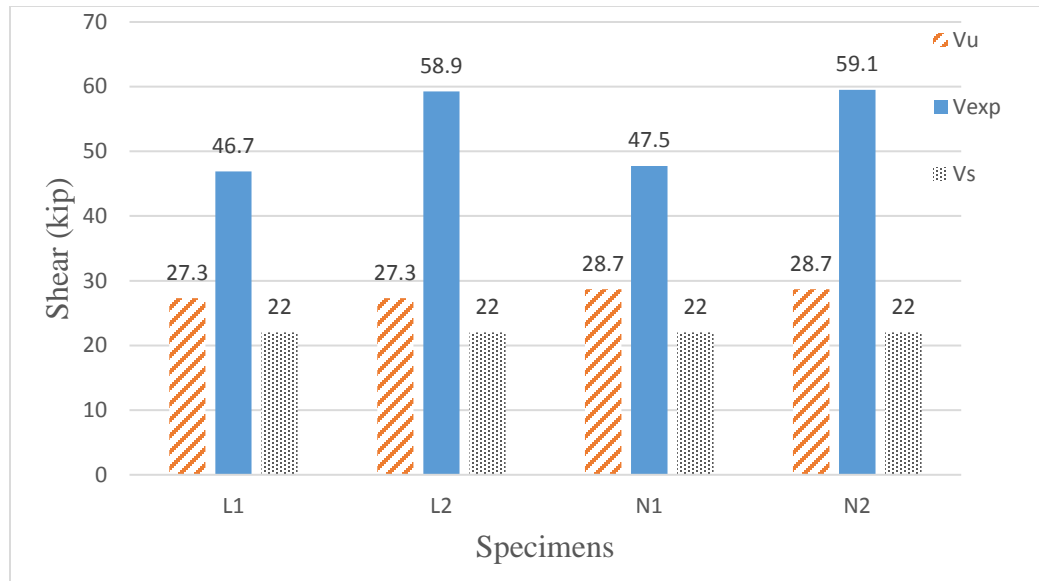
Figure 38. Comparison of experimental shear with the demand in baseline beams

Cracking at the edges of foam

The third and final objective was to evaluate cracking behavior (if any) at the end of the foam void. This was done by using visual observations and strain gage monitoring. This objective was considered during stages one though six; in stage seven the load did not pass through the section in question.

Intuitively, the transition point between the solid and foam-void portions of the specimens was considered as a likely location for cracking. The cross-section changes abruptly at this location and the corners of the foam void were likely locations for stress concentrations. In spite of these conditions, no cracks were observed near the edges of the foam. As was shown previously in the Figure 32, the moment-strain relationship reported by strain gages at the edges of the foam was linear-elastic throughout the flexural load test. Furthermore, no cracks were observed during visual inspections. As with the

concrete contribution to shear capacity, the absence of cracking may have been due to the relatively high concrete strength at the time of testing. The absence of cracking at the edges of the foam during the tests suggested that the concrete strength, foam detail, and reinforcement detail provide adequate resistance to cracking under parking garage load conditions.

VIII.   CONCLUSIONS AND RECOMMENDATIONS

This thesis reports the results of experimental testing of four foam-void precast prestressed tee-beams. The tests were complimented by structural analyses of a "baseline" beam which the specimens were designed to mimic. The baseline beam was a typical 60-ft span precast DT member for a parking garage. The motivation for the research was to reduce the self-weight of parking garage DT members such that two members can be shipped in one load.

The experimental program had three specific objectives:

- Evaluate experimental flexural capacity of FVDT relative to calculated nominal capacity;

- Evaluate experimental shear capacity of FVDT relative to factored shear force in baseline beam; and

- Evaluate cracking behavior (if any) at the end of the foam void.

Test program conclusions

The following conclusions are made with respect to each of the stated objectives:

- The foam-void test specimens supported experimental moments that exceeded theoretical nominal capacity. The ratios of experimental-to-nominal moment capacities were between 1.15 and 1.17. It was concluded that classical flexural theory can be reasonably applied to precast concrete DT members with foam-voids placed in the web.

- The test specimens had significantly more shear capacity than the calculated shear demand of the "baseline" parking garage beam. The experimental shear capacity of the specimens was always greater than two times that of the calculated shear demand. In spite of the foam-voids placed within the web, the concrete contribution to experimental shear capacity was always greater than the calculated contribution from the steel reinforcement.

- Cracking was not observed at the end of the foam voids near the ultimate load levels. Thus, cracking at the foam ends would not be expected in service conditions for similar foam-void DT members.

The above observations are specific to the tested specimens and are conditional on the concrete strength, transverse reinforcement, and other structural details. The minimum compressive strength for any specimens at the time of testing was on an average 9610 psi. Transverse reinforcement consisted of double-leg #3 stirrups spaced at 12 in.

Recommendations for design

When designing foam-void double-tee members, it is recommend that classical flexural theory be applied. The foam voids had no observable influence on the flexural capacity or behavior of the test specimens. Care should be taken, however, if the compression block is interrupted by the foam void or if the void is placed at a location that would interrupt bond between strands and concrete.

Regarding shear design, the shear reinforcement details used in the test program are recommended unless an alternative detail is experimentally validated. The tested foam-void thicknesses (1 in. and 2in.) are recommended for use with the tested shear reinforcement detail. Foam voids should not be placed within 5 ft (approximately two times the beam height) from member ends. Chamfering or curving the edges of the foam boards at the transition to a solid cross section, while not done in the test program, are recommended; this can be easily implemented by cutting the foam boards prior to placement in the webs.

The recommendations do not change with respect to concrete unit weight. The above recommendations apply to FVDT members with reduced-weight and normal-weight concretes.

Recommendations for future testing

The experimental program considered four specimens with variable unit-weight of concrete and thickness of the foam. The member size, strand pattern, reinforcement details, depth of foam void, and length of foam void remained constant. If future tests are to be conducted, the following variables and conditions are recommended:

- Thicker foam voids are recommended for testing. Thickness of the foam in the current test program was on the conservative side. Future tests could "push the limit" of foam thickness to see how far the concept can be taken.
- Deeper foam voids are recommend if deeper members are tested.

- To reduce any effects of stress concentrations at the edges of the foam voids, chamfers or curves of the foam boards are recommended. This wasn't an issue in the current test program, but is unlikely to have any negative impact and can be relativity easily implemented.

- Combinations of foam void thickness and concrete unit weight that are likely to result in two-at-a-time trucking are recommended for testing. Figure 10 can be used as a starting point for selecting variables.

- Concretes having lower compressive strengths are recommended for use in future FDVT test specimens. The compressive strengths in the current program were 9610 psi or greater.

- Alternative shear reinforcement details are suggested for consideration. One possibility is the use of bent wire mesh that sandwiches the foam void (Figure 39). Similar to the concept in the current test program, the bottom bend can anchor the mesh around the prestressed strands. Distinct from the current program, the foam would be anchored to the mesh using tie wire instead of welded cross pieces. This detail would reduce the effort required to make custom stirrups used in the test program. It would also ease the placement of the foam boards because the top cross pieces are replaced by wires that can be installed after the board is in place. This detail would require enough wire ties at the top to prevent the foam from floating upward when the concrete is cast.
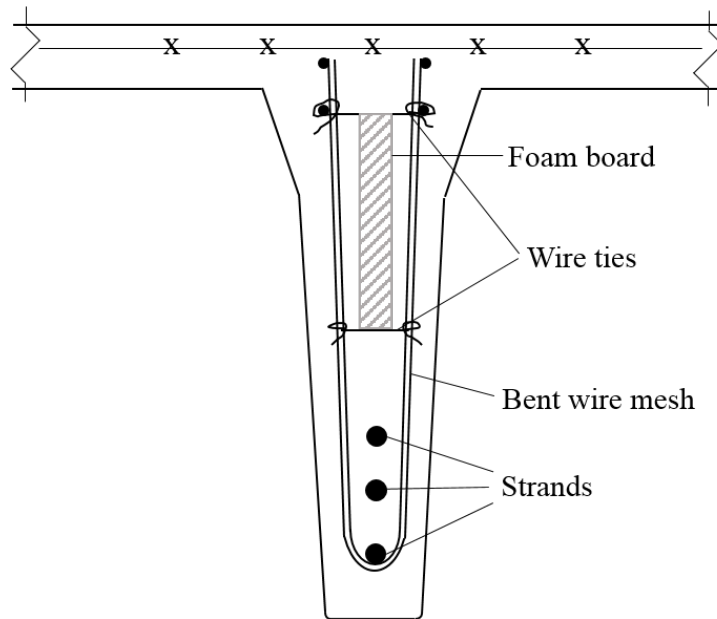
Figure 39. Alternative shear reinforcement recommended

Final Comments

The overall goal was to create a FVDT parking garage members that allowed two-at-a-time trucking. The FVDT test specimens had desirable structural performance, while also having a degree of weight reduction. The weight reducing measures in the test program didn't "push the limits" of the foam void concept, but still provide up to 8% weight reduction relative to a solid DT section. The measures (foam board thickness and concrete unit weight) in the test program may facilitate two-at-a-time trucking in some specific circumstances; however, the variables do not provide sufficient weight reduction associated with the constraints (member size, vehicle weight, GVW limits) associated with typical parking garage members. The thesis author hopes that this work will nevertheless act as a stepping stone from which even lighter FVDT parking garage members may be studied, tested, and implemented.

REFERENCES

1. Nasser, G., Tadros, M., Sevenker A., and Nasser D., "The Legacy and Future of an American Icon: The Precast, Prestressed Concrete Double Tee," *PCI Journal* (2015).

2. Wilden H. "Setting the Record Straight on the Origin of the Prestressed Double Tee" (2014) http://www.enconunited.com/pdf/Double%20Tee%20Origin.pdf Accessed 28 June 2017.

3. Edwards, H., "The Innovators of Prestressed Concrete in Florida." *PCI Journal* (1978).

4. ("PCI Northeast - Projects" n.d.), http://www.pcine.org/projects/project.cfm Accessed 10 November 2017.

5. Barney, G., Corley, W., Hanson, J., and Parmelee, R., "Behavior and Design of Prestressed Concrete Beams with Large Web Openings," *PCI Journal* (1977).

6. Savage, J., Tadros, M., Arumugasaamy, P., and Fischer, L "Behavior and Design of Double Tees with Web Openings," *PCI Journal* (1996).

7. Saleh, M., Tadros, M., Einea, A., Fischer, L., and Foster, E "Standardized Design of Double Tees with Large Web Openings." *PCI Journal*, (1999).

8. BubbleDeck Systems. (2008), http://www.bubbledeck.com/ Accessed 28 June 2017.

9. ASCE. 2010. *Minimum Design Loads for Buildings and Other Structures*. ASCE/SEI Standard 7-10

10. PCI. "PCI Design Handbook 7th Edition" *Precast/Prestressed Concrete Institute* (2010).

11. ACI Committee 318, "*Building Code Requirements for Structural Concrete (ACI 318-14) and Commentary (ACI 318R-14)*," American Concrete Institute, Farmington Hills, MI, 2014, 519 pp.

Baseline beam analysis (NWC)

Section Properties:

$A := 298 \cdot in^2$

$h := 28in$

$hf := 2in$

$bf := 72in$

$L := 60ft$

$n := 5 \quad \text{No of Strands}$

$ds := \dfrac{9}{16}in$

$A_{strand} := 0.191 \cdot in^2$

$Aps := n \cdot A_{strand} = 0.955 \cdot in^2$

$hs := \dfrac{(2 + 4 + 6 + 8 + 10) \cdot in}{5} = 6 \cdot in$

$y_b := 20.5 \cdot in$

$e := y_b - hs = 14.5 \cdot in$

$I := 20655 \cdot in^4$

Material properties:

$fci := 4 \cdot ksi \quad$ initial concrete strength

$fcp := 6 \cdot ksi \quad$ concrete strength after 28 days

$fcf := 4ksi \quad$ concrete strength of topping

$fpu := 270ksi$

$fpi := 180 \cdot ksi \quad$ Elastic losses are considered

$fse := 160ksi \quad$ Total losses are considered

$Ecf := 57ksi \cdot \sqrt{\dfrac{fcf}{psi}} = 3605 \cdot ksi \quad Ecp := 57ksi \cdot \sqrt{\dfrac{fcp}{psi}} = 4415 \cdot ksi$

$$nc := \frac{Ecf}{Ecp} = 0.816$$

$$ybar\_p := y_b = 20.5 \cdot in$$

$$ybar\_f := h - \frac{hf}{2}$$

$$y_t := h - y_b = 7.5 \cdot in$$

$$A := 295 \cdot in^2$$

$$Af := hf \cdot bf \cdot nc = 118 \cdot in^2$$

$$Ac := A + Af = 413 \cdot in^2$$

$$ybar := \frac{Af \cdot ybar\_f + A \cdot ybar\_p}{Ac} = 22.4 \cdot in$$

$$Sb := \frac{I}{y_b} = 1.008 \times 10^3 \cdot in^3$$

$$If := \frac{1}{12} \cdot bf \cdot nc \cdot hf^3 = 39 \cdot in^4$$

$$St := \frac{I}{y_t} = 2.754 \times 10^3 \cdot in^3$$

$$Ic := If + Af \cdot (ybar - ybar\_f)^2 + I + A \cdot (ybar - ybar\_p)^2 = 2.425 \times 10^4 \cdot in^4$$

$$Stf := \frac{Ic}{(h + hf - ybar)} = 3170 \cdot in^3$$

$$Sbf := \frac{Ic}{(h - ybar)} = 4293 \cdot in^3$$

$$Stp := \frac{Ic}{(h - ybar)} = 4293 \cdot in^3$$

$$Sbp := \frac{Ic}{(ybar)} = 1085 \cdot in^3$$

Moment and shear calculations:

w := 6·ft   (Trib. Width)

SDL := 5·psf

Topping := 25·psf

LL := 40·psf

wsd := SDL·w = 30·plf

$w_{topping}$:= Topping·w = 150·plf

wll := LL·w = 240·plf

WTc := 145pcf   Concrete unit weight

wp := A·WTc = 297·plf

$lt := \dfrac{fse}{3000psi}·ds = 2.5\,ft$

wp := A·WTc = 297·plf

W_{DL} := wp + wsd + $w_{topping}$ = 477.049·plf

W_{LL} := wll = 240·plf

$Mop := \dfrac{wp·L^2}{8} = 1.604 \times 10^3·kip·in$

$Mt := \dfrac{w_{topping}·L^2}{8} = 810·kip·in$

$Msd := \dfrac{wsd·L^2}{8} = 162·kip·in$

$Mll := \dfrac{wll·L^2}{8} = 1296·kip·in$

Mser := (Mop + Mt + Msd) + Mll = 322.672·kip·ft

Mu1 := 1.2·(Mop + Mt + Msd) + 1.6·Mll = 430.406·kip·ft

Mu2 := 1.4·(Mop + Mt + Msd) = 300.541·kip·ft

Mu := max(Mu1, Mu2) = 430.406·kip·ft

$$W := W_{DL} + W_{LL} = 717.049 \cdot plf$$

$$V_{DL}(x) := W_{DL} \cdot \frac{L}{2} - W_{DL} \cdot x$$

$$V_{DL}(5 \cdot ft) = 11.926 \cdot kip$$

$$V_{LL}(x) := W_{LL} \cdot \frac{L}{2} - W_{LL} \cdot x$$

$$V_{LL}(5 \cdot ft) = 6 \cdot kip$$

$$Vser(x) := V_{DL}(x) + V_{LL}(x) \qquad Vult(x) := 1.2\,V_{DL}(x) + 1.6\,V_{LL}(x)$$

$$Vser(5 \cdot ft) = 17.926 \cdot kip \qquad\qquad Vult(5 \cdot ft) = 23.911 \cdot kip$$

$$Vser(0 \cdot ft) = 21.511 \cdot kip \qquad\qquad Vult(0 \cdot ft) = 28.694 \cdot kip$$

Stress calculations:

$$Pi := Aps \cdot fpi = 171.9 \cdot kip$$

Losses are considered

$$Pe := Aps \cdot fse = 152.8 \cdot kip$$

$$ftiACI := -6 \cdot \sqrt{fcf \cdot psi} = -379\,psi \qquad \text{Allowable tension in stage 1}$$

$$fciACI := 0.7 \cdot fci = 2800\,psi \qquad \text{Allowable compression in stage 1}$$

$$ftp1 := \frac{Pi}{A} - \frac{Pi \cdot e}{St} + \frac{Mop}{St} = 260.09 \cdot psi$$

$$fbp1 := \frac{Pi}{A} + \frac{Pi \cdot e}{Sb} - \frac{Mop}{Sb} = 1464.53 \cdot psi$$

$$ftp2 := \frac{Pe}{A} - \frac{Pe \cdot e}{St} + \frac{Mop}{St} = 295.91 \cdot psi$$

$$fbp2 := \frac{Pe}{A} + \frac{Pe \cdot e}{Sb} - \frac{Mop}{Sb} = 1124.91 \cdot psi$$

Stress limits at service conditions:

$$fcpACI := 0.6 \cdot fcp = 3600\,psi$$

$$fcfACI := 0.6 \cdot fcf = 2400\,psi$$

$$\text{ftACI} := -7.5 \cdot \sqrt{\text{fcp} \cdot \text{psi}} = -581\,\text{psi} \qquad \text{Class U (uncracked) tension}$$

$$\text{fcACI} := -12 \cdot \sqrt{\text{fcp} \cdot \text{psi}} = -930\,\text{psi} \qquad \text{Class C (cracked) tension}$$

$$\text{ftp3} := \text{ftp2} + \frac{\text{Mt}}{\text{Stp}} = 484.58 \cdot \text{psi}$$

$$\text{fbp3} := \text{fbp2} - \frac{\text{Mt}}{\text{Sbp}} = 378.18 \cdot \text{psi}$$

$$\text{ftc3} := \frac{\text{Mt}}{\text{Stf}} \cdot \text{nc} = 208.60 \cdot \text{psi}$$

$$\text{fbc3} := \frac{\text{Mt}}{\text{Sbf}} \cdot \text{nc} = 154.05 \cdot \text{psi}$$

$$\text{ftp5} := \text{ftp3} + \frac{\text{Msd} + \text{Mll}}{\text{Stp}} = 824.20 \cdot \text{psi}$$

$$\text{fbp5} := \text{fbp3} - \frac{\text{Msd} + \text{Mll}}{\text{Sbp}} = -965.94 \cdot \text{psi}$$

$$\text{ftc5} := \text{ftc3} + \text{nc} \cdot \frac{\text{Msd} + \text{Mll}}{\text{Stf}} = 584.09 \cdot \text{psi}$$

$$\text{fbc5} := \text{fbc3} - \text{nc} \cdot \frac{\text{Msd} + \text{Mll}}{\text{Sbf}} = -123.24 \cdot \text{psi}$$

Baseline beam analysis (LWC)

Section Properties:

$A := 298 \cdot in^2$

$h := 28in$

$hf := 2in$

$bf := 72in$

$L := 60ft$

$n := 5$ No of Strands

$ds := \dfrac{9}{16}in$

$A_{strand} := 0.191 \cdot in^2$

$Aps := n \cdot A_{strand} = 0.955 \cdot in^2$

$hs := \dfrac{(2 + 4 + 6 + 8 + 10) \cdot in}{5} = 6 \cdot in$

$y_b := 20.5 \cdot in$

$e := y_b - hs = 14.5 \cdot in$

$I := 20655 \cdot in^4$

Material properties:

$fci := 4 \cdot ksi$ initial concrete strength

$fcp := 6 \cdot ksi$ concrete strength after 28 days

$fcf := 4ksi$ concrete strength of topping

$fpu := 270ksi$

$fpi := 180 \cdot ksi$ Elastic losses are considered

$fse := 160ksi$ Total losses are considered

$Ecf := 57ksi \cdot \sqrt{\dfrac{fcf}{psi}} = 3605 \cdot ksi$ $Ecp := 57ksi \cdot \sqrt{\dfrac{fcp}{psi}} = 4415 \cdot ksi$

$$nc := \frac{Ecf}{Ecp} = 0.816$$

$$ybar\_p := y_b = 20.5 \cdot in$$

$$ybar\_f := h - \frac{hf}{2}$$

$$y_t := h - y_b = 7.5 \cdot in$$

$$A := 295 \cdot in^2$$

$$Af := hf \cdot bf \cdot nc = 118 \cdot in^2$$

$$Ac := A + Af = 413 \cdot in^2$$

$$ybar := \frac{Af \cdot ybar\_f + A \cdot ybar\_p}{Ac} = 22.4 \cdot in$$

$$Sb := \frac{I}{y_b} = 1.008 \times 10^3 \cdot in^3$$

$$If := \frac{1}{12} \cdot bf \cdot nc \cdot hf^3 = 39 \cdot in^4$$

$$St := \frac{I}{y_t} = 2.754 \times 10^3 \cdot in^3$$

$$Ic := If + Af \cdot (ybar - ybar\_f)^2 + I + A \cdot (ybar - ybar\_p)^2 = 2.425 \times 10^4 \cdot in^4$$

$$Stf := \frac{Ic}{(h + hf - ybar)} = 3170 \cdot in^3$$

$$Sbf := \frac{Ic}{(h - ybar)} = 4293 \cdot in^3$$

$$Stp := \frac{Ic}{(h - ybar)} = 4293 \cdot in^3$$

$$Sbp := \frac{Ic}{(ybar)} = 1085 \cdot in^3$$

Moment and shear calculations:

w := 6·ft   (Trib. Width)

SDL := 5·psf

Topping := 25·psf

LL := 40·psf

wsd := SDL·w = 30·plf

$w_{topping}$:= Topping·w = 150·plf

wll := LL·w = 240·plf

WTc := 126pcf   Concrete unit weight

wp := A·WTc = 258.1·plf

$lt := \dfrac{fse}{3000psi}·ds = 2.5\,ft$

wp := A·WTc = 258.1·plf

W_{DL} := wp + wsd + $w_{topping}$ = 438.125·plf

W_{LL} := wll = 240·plf

$Mop := \dfrac{wp·L^2}{8} = 1.394 \times 10^3·kip·in$

$Mt := \dfrac{w_{topping}·L^2}{8} = 810·kip·in$

$Msd := \dfrac{wsd·L^2}{8} = 162·kip·in$

$Mll := \dfrac{wll·L^2}{8} = 1296·kip·in$

Mser := (Mop + Mt + Msd) + Mll = 305.156·kip·ft

Mu1 := 1.2·(Mop + Mt + Msd) + 1.6·Mll = 409.387·kip·ft

Mu2 := 1.4·(Mop + Mt + Msd) = 276.019·kip·ft

Mu := max(Mu1 , Mu2) = 409.387·kip·ft

68

$W := W_{DL} + W_{LL} = 678.125 \cdot plf$

$V_{DL}(x) := W_{DL} \cdot \dfrac{L}{2} - W_{DL} \cdot x$

$V_{DL}(5 \cdot ft) = 10.953 \cdot kip$

$V_{LL}(x) := W_{LL} \cdot \dfrac{L}{2} - W_{LL} \cdot x$

$V_{LL}(5 \cdot ft) = 6 \cdot kip$

$Vser(x) := V_{DL}(x) + V_{LL}(x)$ $Vult(x) := 1.2\, V_{DL}(x) + 1.6\, V_{LL}(x)$

<mark>$Vser(5 \cdot ft) = 16.953 \cdot kip$</mark>   <mark>$Vult(5 \cdot ft) = 22.744 \cdot kip$</mark>
<mark>$Vser(0 \cdot ft) = 20.344 \cdot kip$</mark>   <mark>$Vult(0 \cdot ft) = 27.293 \cdot kip$</mark>

Stress calculations:

$Pi := Aps \cdot fpi = 171.9 \cdot kip$

                            Losses are considered

$Pe := Aps \cdot fse = 152.8 \cdot kip$

$ftiACI := -6 \cdot \sqrt{fcf \cdot psi} = -379\, psi$ Allowable tension in stage 1

$fciACI := 0.7 \cdot fci = 2800\, psi$ Allowable compression in stage 1

$ftp1 := \dfrac{Pi}{A} - \dfrac{Pi \cdot e}{St} + \dfrac{Mop}{St} = 183.77 \cdot psi$

$fbp1 := \dfrac{Pi}{A} + \dfrac{Pi \cdot e}{Sb} - \dfrac{Mop}{Sb} = 1673.14 \cdot psi$

$ftp2 := \dfrac{Pe}{A} - \dfrac{Pe \cdot e}{St} + \dfrac{Mop}{St} = 219.59 \cdot psi$

$fbp2 := \dfrac{Pe}{A} + \dfrac{Pe \cdot e}{Sb} - \dfrac{Mop}{Sb} = 1333.52 \cdot psi$

Stress limits at service conditions:

$fcpACI := 0.6 \cdot fcp = 3600\, psi$

$fcfACI := 0.6 \cdot fcf = 2400\, psi$

$\text{ftACI} := -7.5 \cdot \sqrt{\text{fcp} \cdot \text{psi}} = -581\,\text{psi}$ Class U (uncracked) tension

$\text{fcACI} := -12 \cdot \sqrt{\text{fcp} \cdot \text{psi}} = -930\,\text{psi}$ Class C (cracked) tension

$$\text{ftp3} := \text{ftp2} + \frac{\text{Mt}}{\text{Stp}} = 408.26 \cdot \text{psi}$$

$$\text{fbp3} := \text{fbp2} - \frac{\text{Mt}}{\text{Sbp}} = 586.79 \cdot \text{psi}$$

$$\text{ftc3} := \frac{\text{Mt}}{\text{Stf}} \cdot \text{nc} = 208.60 \cdot \text{psi}$$

$$\text{fbc3} := \frac{\text{Mt}}{\text{Sbf}} \cdot \text{nc} = 154.05 \cdot \text{psi}$$

$$\text{ftp5} := \text{ftp3} + \frac{\text{Msd} + \text{Mll}}{\text{Stp}} = 747.88 \cdot \text{psi}$$

$$\text{fbp5} := \text{fbp3} - \frac{\text{Msd} + \text{Mll}}{\text{Sbp}} = -757.33 \cdot \text{psi}$$

$$\text{ftc5} := \text{ftc3} + \text{nc} \cdot \frac{\text{Msd} + \text{Mll}}{\text{Stf}} = 584.09 \cdot \text{psi}$$

$$\text{fbc5} := \text{fbc3} - \text{nc} \cdot \frac{\text{Msd} + \text{Mll}}{\text{Sbf}} = -123.24 \cdot \text{psi}$$
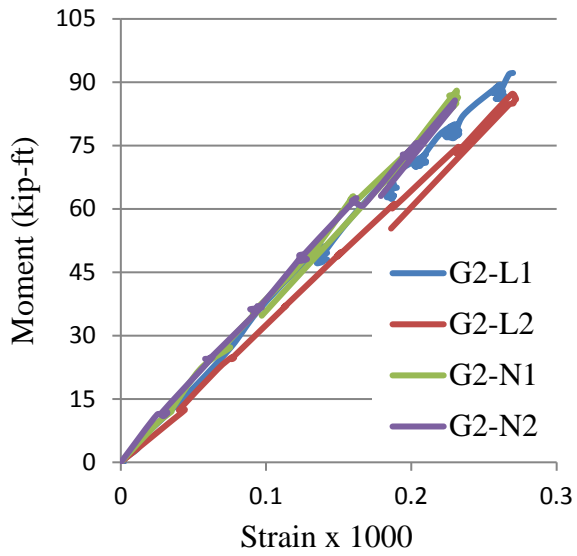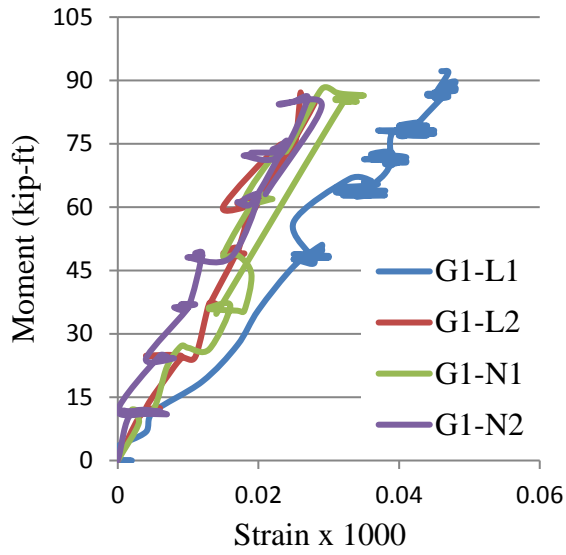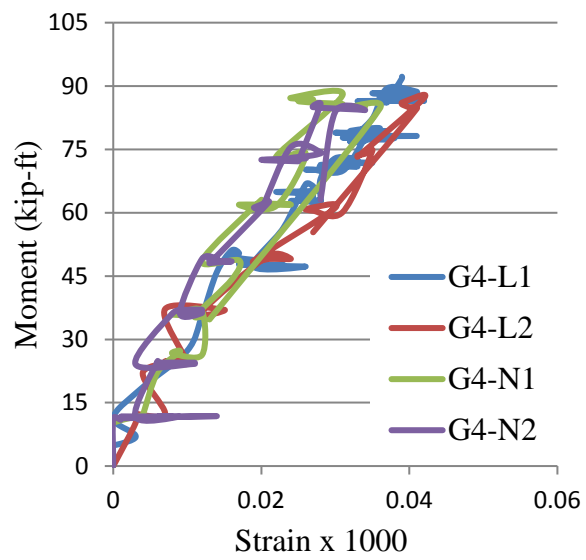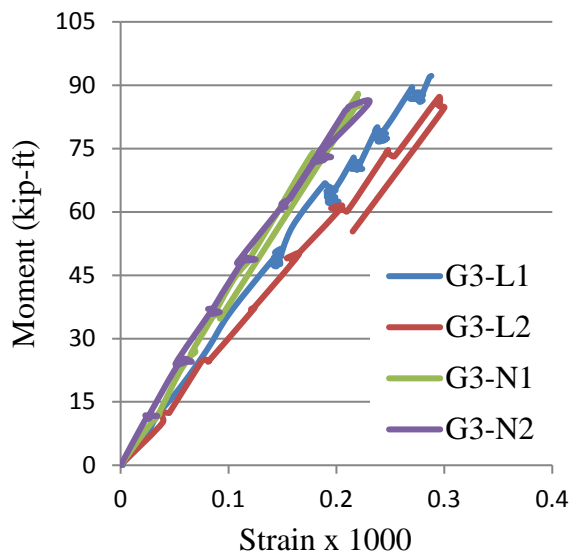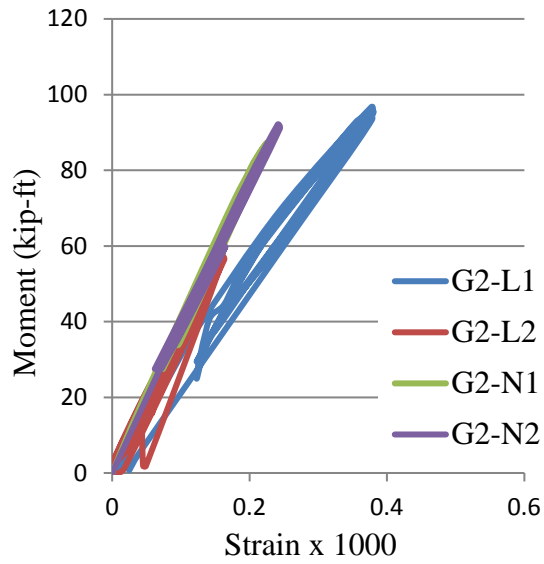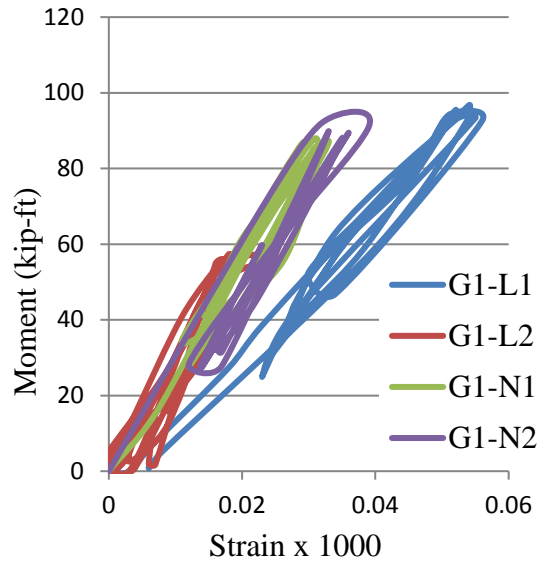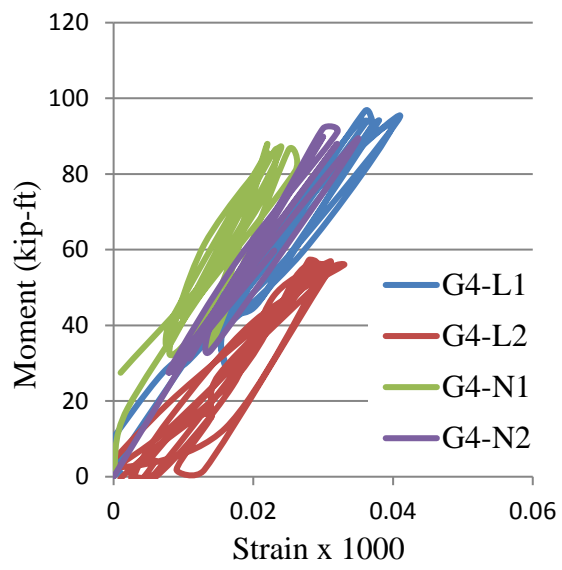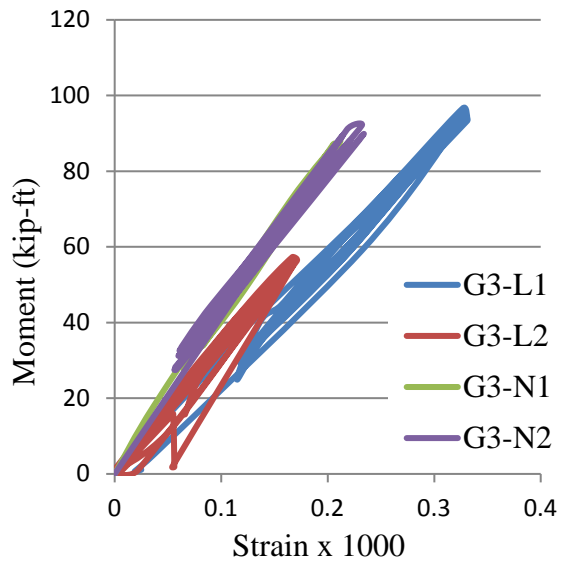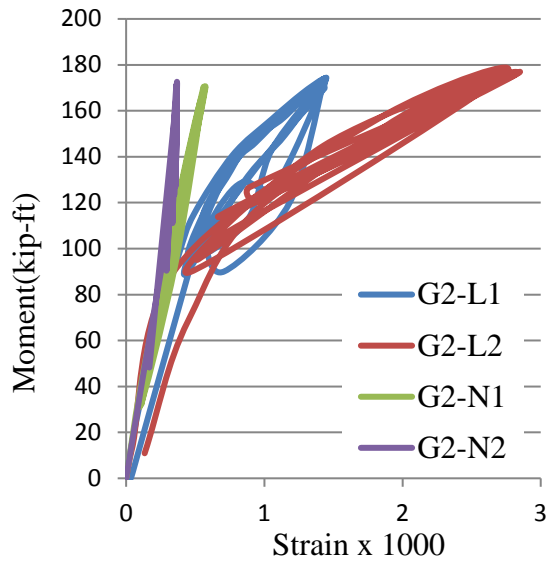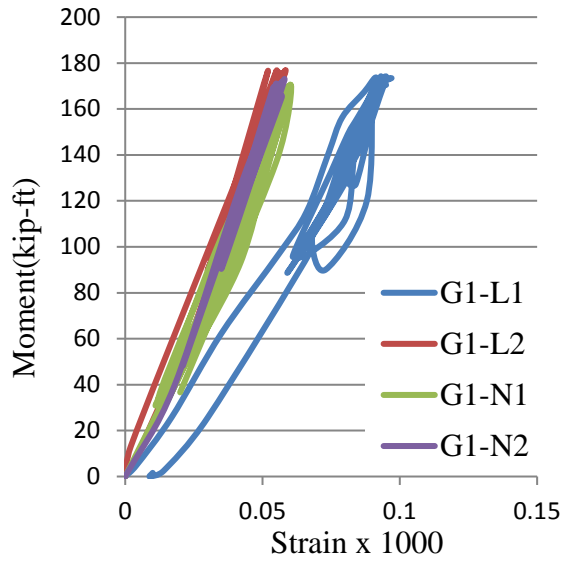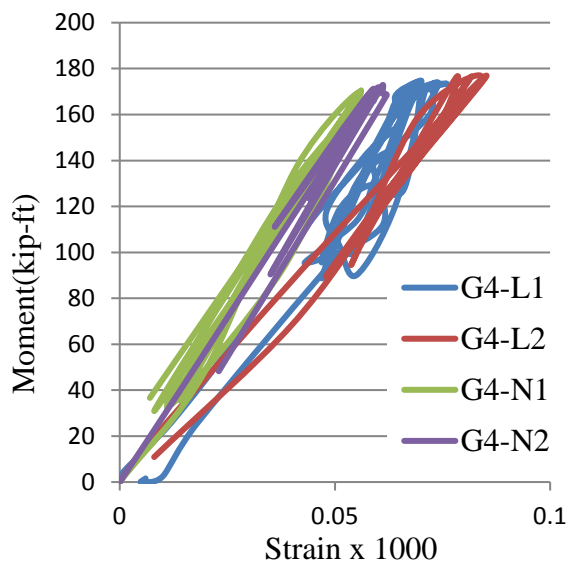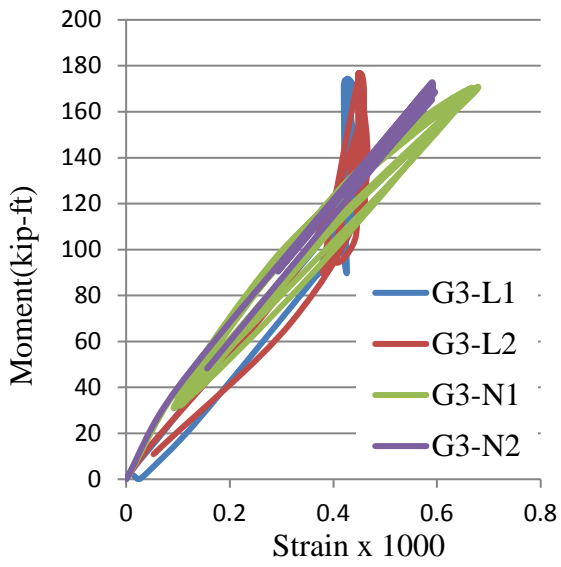
FVDT beams (N1 & N2) analysis:

Section properties:

$A := 298 \cdot in^2$

$L := 35ft$

$hf := 2in$

$bf := 72in$

$h := 28in$

$h_{foam} := 12 \cdot in$

$t_{foam1} := 1 \cdot in$ Foam
                             dimensions
$t_{foam2} := 2 \cdot in$

$bw := 6.25in$

$hs := 4in$

$d_p := h - hs = 24 \cdot in$ Depth of
                                  prestressing strands

$y_b := 20.5 \cdot in$

$e := y_b - hs = 16.5 \cdot in$ eccentricity

$n := 3$ No of strands $ds := \dfrac{9}{16}in$

$\gamma p := 0.28$ Low-lax strands

$I := 20655 \cdot in^4$

Material properties:

$Aps := 0.573 \cdot in^2$ area of 3 9/16 strands

$fpu := 270ksi$

$fpi := 180ksi$ Elastic losses are considered

$fse := 160ksi$ Total losses are considered

$f'ci := 3.5 \cdot ksi$ $f'c := 9.380 \cdot ksi$

$$Eci := 57ksi \cdot \sqrt{\frac{f'ci}{psi}} = 3372 \cdot ksi \quad \text{Concrete elastic modulus at transfer}$$

$$Ec := 57ksi \cdot \sqrt{\frac{f'c}{psi}} = 5520 \cdot ksi \quad \text{Concrete modulus after 28 days}$$

$$E_s := 28500 \cdot ksi \quad \text{Elastic modulus of prestressing strands}$$

$$y_t := h - y_b = 7.5 \cdot in$$

$$Sb := \frac{I}{y_b} = 1.008 \times 10^3 \cdot in^3$$

$$St := \frac{I}{y_t} = 2.754 \times 10^3 \cdot in^3$$

Moment and shear calculations:

$$w := 6 \cdot ft \quad (Trib. Width)$$

$$SDL := 0 \cdot psf$$

$$Topping := 0 \cdot psf$$

$$LL := 0 \cdot psf$$

$$\gamma_{NWC} := 145pcf$$

$$wsd := SDL \cdot w = 0 \cdot plf$$

$$w_{topping} := Topping \cdot w = 0 \cdot plf$$

$$wll := LL \cdot w = 0 \cdot plf$$

$$lt := \frac{fse}{3000psi} \cdot ds = 2.5 ft$$

$$A_{red\_1} := A - h_{foam} \cdot t_{foam1} = 286 \cdot in^2$$

Reduced areas
respectively for N1 & N2

$$A_{red\_2} := A - h_{foam} \cdot t_{foam2} = 274 \cdot in^2$$

$$w_{swN1} := A_{red\_1} \cdot \gamma_{NWC} = 288 \cdot plf$$

$$w_{swN2} := A_{red\_2} \cdot \gamma_{NWC} = 275.9 \cdot plf$$

$$Msw\_N1(x) := \frac{w_{swN1} \cdot x \cdot (L - x)}{2}$$

$$Msw\_N2(x) := \frac{w_{swN2} \cdot x \cdot (L - x)}{2}$$

$$M_P(x, P) := \begin{vmatrix} \left(\dfrac{P}{2} \cdot x\right) & \text{if } 0ft \le x \le 12.5ft \\[2em] \dfrac{P}{2} \cdot (L - x) & \text{if } 22.5ft \le x \le 35ft \\[2em] \left(\dfrac{P}{2} \cdot 12.5ft\right) & \text{otherwise} \end{vmatrix}$$

$$Mt := \frac{w_{topping} \cdot L^2}{8} = 0 \cdot kip \cdot in \quad M_{P\_N1max} := M_P(17.5ft, 50.3kip) = 314.375 \cdot kip \cdot ft$$

50.3 kip is the max force applied during test stage 6 for N

$$Msd := \frac{wsd \cdot L^2}{8} = 0 \cdot kip \cdot in \quad M_{P\_N2max} := M_P(17.5ft, 51.1kip) = 319.375 \cdot kip \cdot ft$$

51.1 kip is the max force applied during test stage 6 for N

$$Mll := \frac{wll \cdot L^2}{8} = 0 \cdot kip \cdot in$$

$$Msw\_N1(12.5ft) = 40.498 \cdot kip \cdot ft \qquad Msw\_N2(12.5ft) = 38.799 \cdot kip \cdot ft$$

$$Msw\_N1(17.5ft) = 44.098 \cdot kip \cdot ft \qquad Msw\_N2(17.5ft) = 42.248 \cdot kip \cdot ft$$

$$Mu_{swN1} := Msw\_N1(17.5ft) + Mt + Msd = 44.098 \cdot kip \cdot ft$$

$$Mu_{swN2} := Msw\_N2(17.5ft) + Mt + Msd = 42.248 \cdot kip \cdot ft$$

$$M_{uN1} := Mu_{swN1} + M_P(17.5ft, 50.3kip) = 358.473 \cdot kip \cdot ft$$

$$M_{uN2} := Mu_{swN2} + M_P(17.5ft, 51.1kip) = 361.623 \cdot kip \cdot ft$$

$$w_P(P) := \frac{P}{2}$$

$$w_{SDL} := 0$$

$$V_{SWN1}(x) := w_{swN1} \cdot \frac{L}{2} - w_{swN1} \cdot x$$

$$V_{SWN2}(x) := w_{swN2} \cdot \frac{L}{2} - w_{swN2} \cdot x$$

$$V_P(x,P) := \begin{cases} \dfrac{P}{2} & \text{if } 0ft \le x \le 12.5ft \\[2mm] \dfrac{P}{2} & \text{if } 22.5ft \le x \le 35ft \\[2mm] 0 & \text{otherwise} \end{cases}$$

Service shear:

$$V_{uN1}(x,P) := V_{SWN1}(x) + V_P(x,P)$$

$$V_{uN1}(5ft, 28kip) = 17.6\,kip$$

$$V_{uN2}(x,P) := V_{SWN2}(x) + V_P(x,P)$$

$$V_{uN2}(5ft, 28kip) = 17.449\,kip$$

$$V_{uN1}(0ft, 85kip) = 47.54 \cdot kip$$ <---85 kip is the max load applied during test stage 7

$$V_{uN2}(0ft, 108.5kip) = 59.078 \cdot kip$$ <---108.5 kip is the max load applied during test stage 7

Stress calculations:

Max moment is considered among N1 and N2 for stress calculations

$$Pi := Aps \cdot fpi = 103.14 \cdot kip$$

Losses are considered

$$Pe := Aps \cdot fse = 91.68 \cdot kip$$

$$f_{minACI} := -6 \cdot \sqrt{f'c \cdot psi} = -581\,psi \quad \text{Allowable tension in stage 1}$$

$$f_{maxACI} := 0.7 \cdot f'ci = 2450\,psi \quad \text{Allowable compression in stage 1}$$

Stress limits at service conditions:

$$f_{Comp} := 0.6 \cdot f'c = 5628\,psi$$

$$ftACI := -7.5 \cdot \sqrt{f'c \cdot psi} = -726\,psi \qquad \text{Class U (uncracked) Tension}$$

$$fcACI := -12 \cdot \sqrt{f'c \cdot psi} = -1162\,psi \qquad \text{Class C (cracked) Tension}$$

$$ftp1 := \frac{Pi}{A} - \frac{Pi \cdot e}{St} + \frac{Msw\_N1(17.5ft)}{St} = -79.69\,psi$$

$$fbp1 := \frac{Pi}{A} + \frac{Pi \cdot e}{Sb} - \frac{Msw\_N1(17.5ft)}{Sb} = 1509.94\,psi$$

$$ftp2 := \frac{Pe}{A} - \frac{Pe \cdot e}{St} + \frac{Msw\_N1(17.5ft)}{St} = -49.48\,psi$$

$$fbp2 := \frac{Pe}{A} + \frac{Pe \cdot e}{Sb} - \frac{Msw\_N1(17.5ft)}{Sb} = 1283.82\,psi$$

Service stresses at mid span:

$$ftp3 := ftp2 + \frac{M_P(17.5ft,28kip)}{St} = 713.04\,psi$$

$$fbp3 := fbp2 - \frac{M_P(17.5ft,28kip)}{Sb} = -800.43\,psi \qquad \text{Class Transition}$$

Specimen capacity calculations:

$fse = 160 \cdot ksi$ Effective prestress

$$f_{psPCI}(\varepsilon) := \begin{vmatrix} f_{ps} \leftarrow E_s \cdot \varepsilon & \text{if } \varepsilon \leq 0.0085 \\ f_{ps} \leftarrow \left(270 - \dfrac{0.04}{\varepsilon - 0.007}\right) ksi & \text{if } \varepsilon > 0.0085 \\ \text{return } f_{ps} \end{vmatrix}$$

$\varepsilon_{cu} := 0.003$ Ultimate strain in concrete

$\varepsilon_{ps}(c) := \varepsilon_{cu} \cdot \left(\dfrac{d_p - c}{c}\right) + \dfrac{fse}{E_s}$ Strain in strands corresponding to fps

$$\beta_1 := \begin{vmatrix} 0.85 & \text{if } 2500psi \leq f'c \leq 4000psi \\ \left[0.85 - 0.05 \cdot \dfrac{\left(\dfrac{f'c}{psi} - 4000\right)}{1000}\right] & \text{if } 4000psi < f'c < 8000psi \\ 0.65 & \text{otherwise} \end{vmatrix} \quad = 0.65$$

$c_{na} := 0.5in$

$a(c_{na}) := \beta_1 \cdot c_{na}$

$b_w := 4.3in$ $hf = 2 \cdot in$ $l_c := 72in - 4.3$ $L = 35\,ft$

$b_{eff} := \min\left(\dfrac{L}{12}, 16 \cdot hf + b_w, l_c + b_w\right) = 35 \cdot in$

$C_c(c_{na}) := 0.85 \cdot f'c \cdot a(c_{na}) \cdot b_{eff}$ Compression in concrete

$T_{ps}(c_{na}) := Aps \cdot f_{psPCI}(\varepsilon_{ps}(c_{na}))$ Tension in prestressing strands

$Error(c_{na}) := C_c(c_{na}) - T_{ps}(c_{na})$

$c_{act} := root(Error(c_{na}), c_{na}) = 0.851 \cdot in$ Solving for c using 'root' command

$c_{act} = 0.851 \cdot in$ The actual depth of neutral axis

At equilibrium,

$$T_{ps}(c_{act}) = 154.424 \cdot kip \quad \text{and} \quad C_c(c_{act}) = 154.424 \cdot kip$$

$$\phi := \begin{vmatrix} 0.65 & \text{if } \varepsilon_{ps}(c_{act}) \leq 0.002 \\ \\ 0.65 + \left(\varepsilon_{ps}(c_{act}) - 0.002\right) \cdot \dfrac{250}{3} & \text{if } 0.002 < \varepsilon_{ps}(c_{act}) < 0.005 \\ \\ 0.90 & \text{otherwise} \end{vmatrix} \quad = 0.9$$

The moment capacity is given by the following equation,

$$Mn := T_{ps}(c_{act}) \cdot \left(d_p - \frac{\beta_1 \cdot c_{act}}{2} \right) = 305.288 \cdot kip \cdot ft \quad \text{for both N1 and N2}$$

FVDT beams (L1 & L2) analysis:

Section properties:

$A := 298 \cdot in^2$

$L := 35ft$

$hf := 2in$

$bf := 72in$

$h := 28in$

$h_{foam} := 12 \cdot in$

$t_{foam1} := 1 \cdot in$ Foam dimensions

$t_{foam2} := 2 \cdot in$

$hs := 4in$

$d_p := h - hs = 24 \cdot in$ Depth of prestressing strands

$y_b := 20.5 \cdot in$

$e := y_b - hs = 16.5 \cdot in$ eccentricity

$n := 3$ No of strands $ds := \frac{9}{16}in$

$\gamma p := 0.28$ Low-lax strands

$I := 20655 \cdot in^4$

Material properties:

$Aps := 0.573 \cdot in^2$ area of 3 9/16 strands

$fpu := 270ksi$

$fpi := 180ksi$ Elastic losses are considered

$fse := 160ksi$ Total losses are considered

$f'ci := 3.5 \cdot ksi$ $f'c := 9.879 \cdot ksi$

$$\mathrm{Eci} := 57\mathrm{ksi} \cdot \sqrt{\frac{\mathrm{f'ci}}{\mathrm{psi}}} = 3372 \cdot \mathrm{ksi} \quad \text{Concrete elastic modulus at transfer}$$

$$\mathrm{Ec} := 57\mathrm{ksi} \cdot \sqrt{\frac{\mathrm{f'c}}{\mathrm{psi}}} = 5665 \cdot \mathrm{ksi} \quad \text{Concrete modulus after 28 days}$$

$$E_s := 28500 \cdot \mathrm{ksi} \quad \text{Elastic modulus of prestressing strands}$$

$$y_t := h - y_b = 7.5 \cdot \mathrm{in}$$

$$\mathrm{Sb} := \frac{I}{y_b} = 1.008 \times 10^3 \cdot \mathrm{in}^3$$

$$\mathrm{St} := \frac{I}{y_t} = 2.754 \times 10^3 \cdot \mathrm{in}^3$$

Moment and shear calculations:

$$w := 6 \cdot \mathrm{ft} \quad \text{(Trib.Width)}$$

$$\mathrm{SDL} := 0 \cdot \mathrm{psf}$$

$$\mathrm{Topping} := 0 \cdot \mathrm{psf}$$

$$\mathrm{LL} := 0 \cdot \mathrm{psf}$$

$$\gamma_{\mathrm{LWC}} := 126\mathrm{pcf}$$

$$\mathrm{wsd} := \mathrm{SDL} \cdot w = 0 \cdot \mathrm{plf}$$

$$w_{\mathrm{topping}} := \mathrm{Topping} \cdot w = 0 \cdot \mathrm{plf}$$

$$\mathrm{wll} := \mathrm{LL} \cdot w = 0 \cdot \mathrm{plf}$$

$$\mathrm{lt} := \frac{\mathrm{fse}}{3000\mathrm{psi}} \cdot \mathrm{ds} = 2.5\,\mathrm{ft}$$

$$A_{\mathrm{red\_1}} := A - h_{\mathrm{foam}} \cdot t_{\mathrm{foam1}} = 286 \cdot \mathrm{in}^2$$

Reduced areas respectively for N1 & N2

$$A_{\mathrm{red\_2}} := A - h_{\mathrm{foam}} \cdot t_{\mathrm{foam2}} = 274 \cdot \mathrm{in}^2$$

$$w_{swL1} := A_{red\_1} \cdot \gamma_{LWC} = 250.3 \cdot plf$$

$$w_{swL2} := A_{red\_2} \cdot \gamma_{LWC} = 239.7 \cdot plf$$

$$Msw\_L1(x) := \frac{w_{swL1} \cdot x \cdot (L - x)}{2}$$

$$Msw\_L2(x) := \frac{w_{swL2} \cdot x \cdot (L - x)}{2}$$

$$M_P(x,P) := \begin{vmatrix} \left(\dfrac{P}{2} \cdot x\right) & \text{if } 0ft \le x \le 12.5ft \\[2mm] \dfrac{P}{2} \cdot (L - x) & \text{if } 22.5ft \le x \le 35ft \\[2mm] \left(\dfrac{P}{2} \cdot 12.5ft\right) & \text{otherwise} \end{vmatrix}$$

$$Mt := \frac{w_{topping} \cdot L^2}{8} = 0 \cdot kip \cdot in \qquad M_{P\_L1max} := M_P(17.5ft, 51.2kip) = 320 \cdot kip \cdot ft$$

51.2 kip is the max force applied during test stage 6 for L

$$Msd := \frac{wsd \cdot L^2}{8} = 0 \cdot kip \cdot in \qquad M_{P\_L2max} := M_P(17.5ft, 50.3kip) = 314.375 \cdot kip \cdot ft$$

50.3 kip is the max force applied during test stage 6 for L2

$$Mll := \frac{wll \cdot L^2}{8} = 0 \cdot kip \cdot in$$

$$Msw\_L1(12.5ft) = 35.191 \cdot kip \cdot ft \qquad Msw\_L2(12.5ft) = 33.715 \cdot kip \cdot ft$$

$$Msw\_L1(17.5ft) = 38.32 \cdot kip \cdot ft \qquad Msw\_L2(17.5ft) = 36.712 \cdot kip \cdot ft$$

$$Mu_{swL1} := Msw\_L1(17.5ft) + Mt + Msd = 38.32 \cdot kip \cdot ft$$

$$Mu_{swL2} := Msw\_L2(17.5ft) + Mt + Msd = 36.712 \cdot kip \cdot ft$$

$$M_{uL1} := Mu_{swL1} + M_P(17.5ft, 51.2kip) = 358.32 \cdot kip \cdot ft$$

$$M_{uL2} := Mu_{swL2} + M_P(17.5ft, 50.3kip) = 351.087 \cdot kip \cdot ft$$

$$w_P(P) := \frac{P}{2}$$

$$w_{SDL} := 0$$

$$V_{SWL1}(x) := w_{swL1} \cdot \frac{L}{2} - w_{swL1} \cdot x$$

$$V_{SWL2}(x) := w_{swL2} \cdot \frac{L}{2} - w_{swL2} \cdot x$$

$$V_P(x,P) := \begin{vmatrix} \frac{P}{2} & \text{if } 0\text{ft} \le x \le 12.5\text{ft} \\[2mm] \frac{P}{2} & \text{if } 22.5\text{ft} \le x \le 35\text{ft} \\[2mm] 0 & \text{otherwise} \end{vmatrix}$$

Service Shear:

$$V_{uL1}(x,P) := V_{SWL1}(x) + V_P(x,P) \qquad V_{uL1}(5\text{ft}, 28\text{kip}) = 17.128\,\text{kip}$$

$$V_{uL2}(x,P) := V_{SWL2}(x) + V_P(x,P) \qquad V_{uL2}(5\text{ft}, 28\text{kip}) = 16.997\,\text{kip}$$

$$V_{uL1}(0\text{ft}, 84.7\text{kip}) = 46.729 \cdot \text{kip} \qquad \text{<---84.7 kip is the max load applied during test stage 7}$$

$$V_{uL2}(0\text{ft}, 109.4\text{kip}) = 58.896 \cdot \text{kip} \qquad \text{<---109.4 kip is the max load applied during test stage 7}$$

Stress calculations:

Max moment is considered among N1 and N2 for stress calculations

$$Pi := Aps \cdot fpi = 103.14 \cdot \text{kip}$$

Losses are considered

$$Pe := Aps \cdot fse = 91.68 \cdot \text{kip}$$

$$f_{minACI} := -6 \cdot \sqrt{f'c \cdot psi} = -596\,\text{psi} \qquad \text{Allowable tension in stage 1}$$

$$f_{maxACI} := 0.7 \cdot f'ci = 2450\,\text{psi} \qquad \text{Allowable compression in stage 1}$$

87

Stress limits at service conditions:

$$f_{Comp} := 0.6 \cdot f'c = 5927.4 \, psi$$

$$ftACI := -7.5 \cdot \sqrt{f'c \cdot psi} = -745 \, psi \qquad \text{Class U (uncracked) Tension}$$

$$fcACI := -12 \cdot \sqrt{f'c \cdot psi} = -1193 \, psi \qquad \text{Class C (cracked) Tension}$$

$$ftp1 := \frac{Pi}{A} - \frac{Pi \cdot e}{St} + \frac{Msw\_L1(17.5ft)}{St} = -104.86 \, psi$$

$$fbp1 := \frac{Pi}{A} + \frac{Pi \cdot e}{Sb} - \frac{Msw\_L1(17.5ft)}{Sb} = 1578.76 \, psi$$

$$ftp2 := \frac{Pe}{A} - \frac{Pe \cdot e}{St} + \frac{Msw\_L1(17.5ft)}{St} = -74.66 \, psi$$

$$fbp2 := \frac{Pe}{A} + \frac{Pe \cdot e}{Sb} - \frac{Msw\_L1(17.5ft)}{Sb} = 1352.64 \, psi$$

Service stresses at mid span:

$$ftp3 := ftp2 + \frac{M_P(17.5ft, 28kip)}{St} = 687.87 \, psi$$

$$fbp3 := fbp2 - \frac{M_P(17.5ft, 28kip)}{Sb} = -731.61 \, psi \qquad \text{Class Transition}$$

Specimen capacity calculations:

$$fse = 160 \cdot ksi \qquad \text{Effective prestress}$$

$$f_{psPCI}(\varepsilon) := \begin{vmatrix} f_{ps} \leftarrow E_s \cdot \varepsilon & \text{if } \varepsilon \leq 0.0085 \\[2mm] f_{ps} \leftarrow \left(270 - \dfrac{0.04}{\varepsilon - 0.007}\right) ksi & \text{if } \varepsilon > 0.0085 \\[2mm] \text{return } f_{ps} \end{vmatrix}$$

$$\varepsilon_{cu} := 0.003 \qquad\qquad\qquad \text{Ultimate strain in concrete}$$

$$\varepsilon_{ps}(c) := \varepsilon_{cu} \cdot \left(\frac{d_p - c}{c}\right) + \frac{fse}{E_s} \qquad \text{Strain in strands corresponding to fps}$$

$$\beta_1 := \begin{vmatrix} 0.85 & \text{if } 2500psi \leq f'c \leq 4000psi & \qquad = 0.65 \\[2mm] \left[0.85 - 0.05 \cdot \dfrac{\left(\dfrac{f'c}{psi} - 4000\right)}{1000} \right] & \text{if } 4000psi < f'c < 8000psi \\[2mm] 0.65 & \text{otherwise} \end{vmatrix}$$

$$c_{na} := 0.5in$$

$$a(c_{na}) := \beta_1 \cdot c_{na}$$

$$b_w := 4.3in \quad hf = 2 \cdot in \quad l_c := 72in - 4.3 \quad L = 35\,ft$$

$$b_{eff} := \min\left(\frac{L}{12}, 16 \cdot hf + b_w, l_c + b_w\right) = 35 \cdot in$$

$$C_c(c_{na}) := 0.85 \cdot f'c \cdot a(c_{na}) \cdot b_{eff} \qquad \text{Compression in concrete}$$

$$T_{ps}(c_{na}) := Aps \cdot f_{psPCI}(\varepsilon_{ps}(c_{na})) \qquad \text{Tension in prestressing strands}$$

$$Error(c_{na}) := C_c(c_{na}) - T_{ps}(c_{na})$$

$$c_{act} := root(Error(c_{na}), c_{na}) = 0.808 \cdot in \qquad \text{Solving for c using 'root' command}$$

$$c_{act} = 0.808 \cdot in \qquad\qquad\qquad \text{The actual depth of neutral axis}$$

89

At equilibrium,

$T_{ps}(c_{act}) = 154.439 \cdot kip$ and $C_c(c_{act}) = 154.439 \cdot kip$

$$\phi := \begin{vmatrix} 0.65 & \text{if } \varepsilon_{ps}(c_{act}) \leq 0.002 \\[2mm] 0.65 + \left(\varepsilon_{ps}(c_{act}) - 0.002\right) \cdot \dfrac{250}{3} & \text{if } 0.002 < \varepsilon_{ps}(c_{act}) < 0.005 \\[2mm] 0.90 & \text{otherwise} \end{vmatrix} \qquad = 0.9$$

The moment capacity is given by the following equation,

$$Mn := T_{ps}(c_{act}) \cdot \left(d_p - \frac{\beta_1 \cdot c_{act}}{2}\right) = 305.497 \cdot kip \cdot ft \qquad \text{for both L1 and L2}$$